




The fungal pathogen *Ustilago maydis* targets the maize corepressor RELK2 to modulate host transcription for tumorigenesis

Luyao Huang¹, Bilal Ökmen², Sara Christina Stolze³, Melanie Kastl^{1,4}, Mamoona Khan⁵, Daniel Hilbig^{1,4}, Hirofumi Nakagami^{3,6} , Armin Djamei⁵  and Gunther Doehle¹ 

¹Institute for Plant Sciences and Cluster of Excellence on Plant Sciences (CEPLAS), University of Cologne, Cologne, 50674, Germany; ²Department of Microbial Interactions, IMIT/ZMBP, University of Tübingen, Tübingen, 72076, Germany; ³Protein Mass Spectrometry, Max-Planck Institute for Plant Breeding Research, Cologne, 50829, Germany; ⁴Department of Oncology, Hematology and Rheumatology, University Hospital Bonn, Bonn, 53127, Germany; ⁵Department of Plant Pathology, Institute of Crop Science and Resource Conservation (INRES), University of Bonn, Bonn, 53115, Germany; ⁶Basic Immune System of Plants, Max Planck Institute for Plant Breeding Research, Cologne, 50829, Germany

Summary

Author for correspondence:
Gunther Doehle
Email: g.doehle@uni-koeln.de

Received: 14 June 2023
Accepted: 8 November 2023

New Phytologist (2024) 241: 1747–1762
doi: 10.1111/nph.19448

Key words: APETALA2/ethylene-responsive factor transcription factors, EAR motifs, effector protein, TOPLESS, *Ustilago maydis*.

- *Ustilago maydis* is a biotrophic fungus that causes tumor formation on all aerial parts of maize. *U. maydis* secretes effector proteins during penetration and colonization to successfully overcome the plant immune response and reprogram host physiology to promote infection.
- In this study, we functionally characterized the *U. maydis* effector protein Topless (TPL) interacting protein 6 (Tip6). We found that Tip6 interacts with the N-terminus of RELK2 through its two Ethylene-responsive element binding factor-associated amphiphilic repression (EAR) motifs. We show that the EAR motifs are essential for the virulence function of Tip6 and critical for altering the nuclear distribution pattern of RELK2.
- We propose that Tip6 mimics the recruitment of RELK2 by plant repressor proteins, thus disrupting host transcriptional regulation. We show that a large group of AP2/ERF B1 subfamily transcription factors are misregulated in the presence of Tip6.
- Our study suggests a regulatory mechanism where the *U. maydis* effector Tip6 utilizes repressive domains to recruit the corepressor RELK2 to disrupt the transcriptional networks of the host plant.

Introduction

Ustilago maydis, the causal agent of common corn smut, induces tumor formation in various aerial parts of maize (*Zea mays*). To establish successful infection, *U. maydis* employs a diverse array of effector proteins that facilitate interaction with the host plant and promote disease progression (Schuster *et al.*, 2018). Previous studies have shown that *U. maydis* effectors exhibit organ-specific expression and adaptation during infection, as revealed by comparative transcriptome analysis of infected seedlings, adult leaves, and tassels (Skibbe *et al.*, 2010). Among these effectors, nine have been identified as leaf-specific effectors, playing a crucial role in *U. maydis* virulence specifically in maize leaves (Schilling *et al.*, 2014). For instance, Seedling efficient effector 1 (See1), the first characterized leaf-specific effector protein, interacts with the maize SGT1 protein, leading to the reactivation of host DNA synthesis and direct promotion of tumor formation in bundle sheath cells (Redkar *et al.*, 2015; Matei *et al.*, 2018). Additionally, Erc1 (enzyme required for cell-to-cell extension) has recently been found to have 1,3-glucanase activity, which is required for

fungal cell-to-cell elongation in leaf bundle sheaths (Ökmen *et al.*, 2022). Another leaf-specific effector whose deletion resulted in a significant reduction in tumors is UMAG_11060 (Schilling *et al.*, 2014). However, its molecular function has yet to be clearly determined.

Regulating gene expression is crucial for plant responses to biotic and abiotic stress. The TOPLESS (TPL) and TOPLESS RELATED PROTEIN (TPR) corepressors are involved in major plant hormone signaling, as well as meristem initiation and maintenance developmental pathways (Long *et al.*, 2006; Szemenyei *et al.*, 2008; Gallavotti *et al.*, 2010; Pauwels *et al.*, 2010; Oh *et al.*, 2014; Liu *et al.*, 2019). TPL/TPR proteins are recruited directly or indirectly by DNA-binding transcription factors to suppress the expression of target genes. Transcription factors typically interact with TPL through transcriptional repression motifs, such as the ethylene-responsive factor (ERF)-associated amphiphilic repression (EAR) motif, characterized by the LxLxLx or DLNxxP sequence, which mediates interaction with TPL/TPR (Ohta *et al.*, 2001; Hiratsu *et al.*, 2003; Kagale & Rozwadowski, 2011; Causier *et al.*, 2012; Liu *et al.*, 2019). Notably, the

APETALA2/ethylene-responsive factor (AP2/ERF) superfamily of transcription factors was found to be enriched among the interactors of TPL/TPR proteins (Causier *et al.*, 2012). This superfamily plays an important role in various aspects of plant growth and development, including response to biotic and abiotic stresses, hormone signaling, and pathogen defense (Krishnaswamy *et al.*, 2011; Wang *et al.*, 2011; Koyama *et al.*, 2013; Chandler, 2018; Han *et al.*, 2020). The AP2/ERF superfamily can be further classified into five subfamilies: AP2, ERF, dehydration-responsive element-binding (DREB) proteins, related to abscisic acids-intensive 3/viviparous 1 (RAV), and solist (Sakuma *et al.*, 2002; Cheng *et al.*, 2023).

ERF transcription factors normally interact with a cis-regulatory element known as the GCC box, which comprises the DRE/C-repeat (DRE/CRT) element and the ethylene-responsive element (ERE; Masaru & Hideaki, 1995; Sessa *et al.*, 1995; Büttner & Singh, 1997; Hao *et al.*, 1998; Fujimoto *et al.*, 2000). These factors are commonly found in the promoters of genes that respond to abiotic stress, jasmonate- and ethylene-inducible genes, and genes involved in pathogenesis (Masaru & Hideaki, 1995; Büttner & Singh, 1997; Chakravarthy *et al.*, 2003; Lorenzo *et al.*, 2003; Pré *et al.*, 2008; Maruyama *et al.*, 2013). The ERF family is categorized into six subgroups, designated as B1 to B6, with the B3 family being responsible for regulating multiple disease resistance pathway genes (McGrath *et al.*, 2005; Moffat *et al.*, 2012). Overexpression of AtERF1 resulted in the upregulation of PLANT DEFENSIN1.2 (PDF1.2) and chitinases (Solano *et al.*, 1998; Lorenzo *et al.*, 2003). Similarly, the overexpression of the tomato ERF transcription factor Pti4 stimulated the expression of pathogenesis-related (PR) 1 and PR2, leading to increased resistance against fungal and bacterial pathogens (Gu *et al.*, 2002). The B1 family plays a vital role in plant development, with the *Arabidopsis* gene *PUCHI* contributing to lateral root cell division and floral meristem identity (Hirota *et al.*, 2007; Karim *et al.*, 2009; Bellande *et al.*, 2022). Homologs of *PUCHI*, such as BRANCHED SILKLESS1 (BD1) in maize and FRIZZY PANICLE (FZP)/BRANCHED FLORETLESS1 (BFL1) in rice, are also involved in floral meristem development (Chuck *et al.*, 2002; Komatsu *et al.*, 2003). Moreover, members of the B1 family, including AtERF3 and AtERF4, function as repressors that can downregulate the transcription level of reporter genes and the transactivation activity of transcription factors (Fujimoto *et al.*, 2000; Ohta *et al.*, 2000).

TPL/TPRs serve as important targets for plant pathogens, and several *U. maydis* effectors that target maize TPL proteins have been identified. Maize has four homologs of TPL, RAMOSA1 ENHANCER LOCUS 2 (REL2), and three other REL2-like proteins, RELK1, RELK2, and RELK3 (Liu *et al.*, 2019). Naked1 (Nkd1), a recently discovered effector, interacts with maize TPL through a C-terminal LxLxLx motif. This interaction results in the suppression of pathogen-associated molecular pattern (PAMP)-induced reactive oxygen species (ROS) bursts, leading to a significant decline in plant immunity (Navarrete *et al.*, 2022). Moreover, the Nkd1-TPL interaction hinders TPL recruitment by the Aux/IAA repressor, resulting in the derepression of auxin signaling (Navarrete *et al.*, 2022). The *U. maydis*

cluster gene 6A encodes a family of five effector proteins known as Tips, which play a role in inducing auxin signaling (Bindics *et al.*, 2022). Although neither of them contains an EAR domain, Tip1 and Tip4 compete with the Aux/IAA repressor for TPL binding, ultimately promoting the expression of auxin-responsive genes (Bindics *et al.*, 2022). Additionally, the effector protein Jsi1, through its interaction with maize TPL, promotes the induction of jasmonate/ethylene (JA/ET; Darino *et al.*, 2020). Unlike Nkd1, Jsi1 binds to the second WD40 domain of TPL/TPR proteins via a DLNxxP motif. This interaction enhances the biotrophic susceptibility of *Pst DC3000* in *A. thaliana* by upregulating genes associated with the ERF B3 branch of the JA/ET signaling pathway (Darino *et al.*, 2020). More recently, Topless interacting protein 6 (Tip6), Tip7, and Tip8 were discovered through a large-scale effectors interaction study with maize RELK2, also demonstrating their capacity to induce auxin response (Khan *et al.*, 2023). In this study, we report the functional characterization of the *U. maydis* effector gene *UMAG_11060*, which encodes the Tip6. Tip6 plays a crucial role in the full virulence of *U. maydis*, specifically inducing tumor formation upon seedling infection. We found that Tip6 interacts with maize RELK2 through two EAR motifs, which are required for the virulence function of the effector. Furthermore, Tip6 binds to the N-terminus of RELK2, which alters its subcellular localization. We propose that Tip6 disrupts the regulatory machinery of maize by recruiting RELK2, thus interfering with the expression of maize transcription factors, particularly a group of AP2/ERF B1 subfamily transcription factors. These findings provide valuable insights into the mechanistic aspects of effector-mediated transcriptional regulation modulation in the host.

Materials and Methods

Experimental strains, culture conditions, plant growth conditions, and primer information

Virulence assays used the *U. maydis* strain SG200 and its derivative strains. *U. maydis* strains were grown in YEPS-light liquid medium or on Potato Dextrose Agar (PDA; BD, Franklin Lakes, NJ, USA) plates at 28°C. Plasmid vector cloning utilized *Escherichia coli* Top10 strains, while heterologous protein expression used the *E. coli* BL21 (DE3) strain. Transient protein expression and subcellular observation in *Nicotiana benthamiana* used *Agrobacterium tumefaciens* GV3101 strain. Bacterial strains were cultured in dYT liquid medium or YT agar plates supplemented with suitable antibiotics.

Zea mays Golden Bantam (GB) plants were grown in a glasshouse with controlled conditions of 16 h : 8 h, light : dark, 28°C : 22°C. *N. benthamiana* plants were cultivated in a growth chamber with 16 h : 8 h, light : dark, 22°C. Primer information is provided in Supporting Information Table S1.

Subcellular localization in *N. benthamiana* and maize

Tip6 coding sequence without the signal peptide was fused with mCherry, while RELK2 coding sequence was fused with GFP.

These constructs were transiently expressed in *N. benthamiana* leaves via *Agrobacterium*-mediated transformation. Fluorescence signals were visualized and captured using a Leica SP8 confocal laser scanning microscope (Leica, Wetzlar, Germany). For maize, 6-d-old leaves were bombarded with plasmid-coated gold particles as described (Djamei *et al.*, 2011). Confocal microscopy was performed 16–24 h after transformation.

Yeast two-hybrid assay

The yeast two-hybrid (Y2H) assay followed the Clontech Yeast Protocol Handbook. Tip6 coding sequence and its variants were cloned into the pGBDT7 vector as bait. RELK2 coding sequence and its truncated variants were cloned into either the pGBDT7 or pGADT7 vectors. The resulting pGADT7 and pGBDT7 constructs were transformed into the yeast strain AH109, and the transformed cells were screened on nutrient-deficient plates under different stringency conditions: low stringency (SD-Leu-Trp), medium stringency (SD-Leu-Trp-His), and high-stringency (SD-Leu-Trp-Ade-His). Plates were incubated at 28°C for 4–5 d.

Co-immunoprecipitation and mass spectrometry analysis

Seven-day-old maize seedling leaves were infected with *U. maydis* strains SG200Δ*Tip6-Ppit2::Tip6-3xHA* or SG200-*Ppit2::SP-mCherry-3xHA* following a previously described protocol (Redkar & Dohlemann, 2016). Similarly, *N. benthamiana* plant leaves were infiltrated with *Agrobacterium* strains carrying *p2x35S::GFP* or *p2x35S::Tip6²²⁻²²⁶-GFP*. In both cases, the leaves were harvested at 3 d postinfection (dpi) and ground into powder using liquid nitrogen.

For protein extraction, above ground powder (500 µl) was mixed with 1.5 ml of lysis buffer (50 mM Tris–HCl pH 7.5, 150 mM NaCl, 2 mM EDTA, 10% glycerol, 1% (v/v) Triton X-100, 5 mM dithiothreitol (DTT) and protease inhibitor cocktail (Roche, Cat. no. 04693159001)). After incubation on ice for 30 min, the protein supernatant was obtained by centrifugation twice at 17 000 g, at 4°C for 30 min.

For maize samples, the protein supernatant was incubated with anti-HA magnetic beads (Thermo Fisher, Dreieich, Germany, Cat. no. 88836), while for *N. benthamiana* samples, it was incubated with anti-GFP beads (ChromoTek, Martinsried, Germany, Cat. no. gta). After a 1-h incubation at 4°C, the protein-bound beads were washed and subjected to mass spectrometry analysis.

For maize samples, the beads were re-dissolved in 25 µl digestion buffer 1 (50 mM Tris, pH 7.5, 2 M urea, 1 mM DTT, 5 ng µl⁻¹ trypsin) and incubated at 30°C, 512 g for 30 min. The resulting supernatant was combined with the supernatant obtained after adding 50 µl of digestion buffer 2 (50 mM Tris, pH 7.5, 2 M urea, 5 mM CAA). The supernatants were incubated overnight at 32°C, 512 g in the dark. Digestion was stopped with 1 µl of TFA, and desalting was performed using C18 Empore disk membranes (Rappsilber *et al.*, 2003).

For *N. benthamiana* samples, the beads were eluted with SDT buffer (4% SDS, 100 mM Tris–HCl pH 7.6, 0.1 M DTT) and subjected to the filter-aided sample preparation protocol

(Wiśniewski *et al.*, 2009). The samples were reduced with 1 M DTT, diluted with 8 M urea in 0.1 M Tris/HCl pH 8.5 (UA), and loaded onto filters (Sartorius, Goettingen, Germany, Vivacon 500, VN01H22, 30 kDa cutoff). After washing with UA and alkylating using 100 µl of 55 mM chloroacetamide in UA, the mixture was incubated in the dark for 20 min. Next, 50 µl of LysC solution was added and incubated for 3 h, followed by 300 µl of trypsin solution (1 µg µl⁻¹ trypsin) and incubation overnight. After centrifugation, 50 µl of 50 mM NH₄HCO₃ was added and centrifuged. The resulting peptide-containing flow-through was acidified with TFA and desalted using stage tips with C18 Empore disk membranes (3 M; Rappsilber *et al.*, 2003).

Dried peptides were re-dissolved in 2% ACN, 0.1% TFA. LC–MS/MS analysis was performed using an EASY-nLC 1200 (Thermo Fisher) coupled to a Q Exactive Plus mass spectrometer (Thermo Fisher). Peptides were separated on silica emitters (New Objective, Littleton, CO, USA, 75 µm inner diameter) packed with reversed-phase ReproSil-Pur C18 AQ resin. A total of 0.5 µg of peptides were loaded and eluted over 115 min using a segmented linear gradient of 5–95% solvent (80% ACN, 0.1% FA) at a flow rate of 300 nl min⁻¹. Mass spectra were acquired in data-dependent acquisition mode with the TOP15 method. Peptides with a charge of +1, > 6, or with an unassigned charge state, were excluded from fragmentation, and dynamic exclusion for 30 s prevented repeated selection of precursors.

MS data analysis

For MS data analysis, raw data were processed using MAXQUANT software (v.1.5.7.4; Cox & Mann, 2008) with label-free quantification (LFQ) and iBAQ enabled (Tyanova *et al.*, 2016). MS/MS spectra were searched against a combined database containing *N. benthamiana* or *Z. mays*, along with contaminant proteins and decoy sequences. Search parameters included trypsin specificity, two missed cleavages maximum, and fixed modifications of cysteine residues. Peptide-spectrum-matches and proteins were retained below a false discovery rate of 1%.

Statistical analysis of MaxLFQ values was performed using PERSEUS (v.1.5.8.5). Quantified proteins were filtered based on a sufficient number of valid values in each condition. Two-sample *t*-tests were conducted with a permutation-based FDR of 5%. Missing values were imputed from a normal distribution. The Perseus output was exported and further processed using Excel.

Co-immunoprecipitation in *N. benthamiana*

N. benthamiana plant leaves were infiltrated with *Agrobacterium* carrying the designated constructs. The infiltrated leaves harvested at 2 dpi were ground into powder and mixed with protein extraction buffer. After incubation on ice for 30 min with inversions every 10 min, the samples were centrifuged twice at 4°C for 20 min at 13 000 g. The resulting supernatant was used for a co-immunoprecipitation (Co-IP) assay. For the assays, 1 ml of protein supernatant was incubated with 10 µl of magnetic GFP-Trap beads (ChromoTek, Cat. no. gtma) or magnetic Myc-Trap beads (ChromoTek, Cat. No. yta) at 4°C with constant rotation for

1 h. The beads were washed and resuspended in 80 μ l of 1 \times SDS-loading buffer. After boiling, the samples were analyzed by Western blotting using anti-GFP antibody (Roche, Cat. no. 11814460001) at a dilution of 1 : 1000 and anti-Myc antibody (Sigma, Cat. no. M4439) at a dilution of 1 : 5000.

RNA preparation and RNA-Seq analysis

Maize seedlings infected with *U. maydis* SG200, Δ Tip6, or Tip6EARm were harvested at 3 dpi for total RNA extraction. The infected leaves were ground into powder, and total RNA was extracted using TRIzol Reagent (Invitrogen, Cat. no. 15596018) following the manufacturer's protocol. DNA removal was performed using the Turbo DNA-Free™ Kit (Invitrogen, Cat. no. AM2238) as instructed by the manufacturer. Three independent replicates were collected and subjected to library construction using Illumina NovaSeq 6000 (Illumina) at Novogene (Cambridge, UK). Trim galore (Martin, 2011) was used to remove low-quality reads and adaptors from the RNA-Seq sequences. The trimmed sequences were then mapped to the *Zea mays* B73 reference genome v.5 (Hufford *et al.*, 2021) using STAR, v.2.7.0e (Dobin *et al.*, 2013). Gene counts were calculated using FEATURE-COUNTS (Liao *et al.*, 2014), and genes with counts below 25 in 9 samples were removed, resulting in 29 537 genes kept for analysis. Differentially expressed genes (DEGs) analysis was performed using DESEQ2 (Datasets S1, S2; Love *et al.*, 2014) and EDGER (Datasets S3, S4; Robinson *et al.*, 2010) with cutoff criteria of absolute fold change ≥ 1 and *P*-value < 0.05 . DEGs identified by both DESEQ2 and EDGER (Datasets S5, S6) were subjected to Gene Ontology (GO) term enrichment analysis using SHINYGO v.0.06 (<http://bioinformatics.sdstate.edu/go65/>) (Ge *et al.*, 2020).

Recombinant protein purification and pull-down assay

The *E. coli* BL21 (DE3) strains carrying the designated constructs were cultivated in dYT medium at 30°C until reaching an optical density of 0.6. Protein induction was performed by adding 0.1 mM IPTG and incubating at 18°C for 16–20 h. Cell cultures were collected by centrifugation at 5112 *g* for 20 min at 4°C, and the cell pellets were resuspended in lysis buffer (0.2 M NaH₂PO₄/0.2 M Na₂HPO₄ pH 6.4, 150 mM NaCl, 10 mM imidazole, pH 6.4, 100 μ g ml⁻¹ lysozyme, protease inhibitor tablets), followed by protein extraction using sonication.

The GST-Tip6²²⁻²²⁶-mCherry and GST-mCherry recombinant proteins were purified using glutathione sepharose 4B beads (Cytiva, Dreieich, Germany, Cat. no. 17075601) following the product protocol. The GST tag was removed using PreScission Protease (Thermo Fisher, Cat. no. 88946). The 6xHis-RELK2^N-6xHis recombinant protein was purified using Pierce Ni-NTA resin (QIAGEN, Cat. no. 30210) according to the product protocol. All purified recombinant proteins underwent size-exclusion chromatography (SEC), and the respective protein fractions were collected. The eluted proteins were analyzed using Coomassie brilliant blue (CBB) stained SDS-PAGE gels and Western blots.

For the Co-IP assay, the purified recombinant mCherry or Tip6²²⁻²²⁶-mCherry proteins were separately mixed with purified 6xHis-RELK2^N-6xHis proteins and incubated with pre-washed magnetic mCherry-Trap beads (ChromoTek, Cat. no. rtmak) in wash buffer (0.2 M NaH₂PO₄/0.2 M Na₂HPO₄ pH 6.4, 150 mM NaCl, protease inhibitor tablets) at 4°C for 1 h with rotation. The beads were collected, washed six times with wash buffer, and boiled after adding 100 μ l of 1 \times SDS-loading buffer. The boiled protein samples were analyzed by SDS-PAGE and Western blotting using anti-His antibody (Thermo Fisher, Cat. no. MA1-21315) at a dilution of 1 : 10 000, anti-mCherry antibody (Cell Signaling Technology, Frankfurt am Main, Germany, Cat. no. 6g6) at a dilution of 1 : 3000, and anti-mouse IgG HRP as the second antibody (Cell Signaling Technology, Cat. no. 7076S) at a dilution of 1 : 3000.

Accession numbers

In this study, gene sequences were obtained from the maizeGDB (<https://www.maizegdb.org/>) database. The accession nos. of genes are as follows: RELK1 (Zm00001eb127680), RELK2 (Zm00001eb011010), REL2 (Zm00001eb415530), and RELK3 (Zm00001eb398420).

Results

Tip6 is a secreted effector protein

Tip6 is encoded by the *U. maydis* gene *UMAG_11060*, which was identified as an effector gene with an organ-specific virulence function in maize leaves (Schilling *et al.*, 2014). To assess whether Tip6 is secreted during infection, we generated a *U. maydis* strain that secretes a Tip6-mCherry fusion protein under the control of its native promoter (SG200 Δ Tip6_pTip6::Tip6-mCherry) for subsequent confocal microscopy. To confirm secretion, we used a *U. maydis* strain carrying SG200 Δ pit2_pPit2::Pit2-mCherry as a positive control, which secretes a highly expressed apoplastic Pit2 effector (Mueller *et al.*, 2013). A strain (SG200-pPit2::mCherry) expressing cytoplasmic mCherry driven by the *pit2*-promoter served as a negative control for secretion. Confocal microscopy performed with infected maize leaves revealed that mCherry localizes inside the fungal hyphae, whereas Tip6-mCherry localizes at the periphery of the fungal hyphae, particularly at the hyphae tips, which is similar to the localization of Pit2-mCherry (Fig. 1a). To further examine secretion, we expanded the apoplastic space of infected maize cell by inducing plasmolysis through treatment with 1 M NaCl. This showed that the secreted Tip6-mCherry and Pit2-mCherry, but not cytoplasmic mCherry, accumulate in the apoplastic space of infected maize cells (Fig. 1b). Next, we assessed Tip6 subcellular localization upon *Agrobacterium*-mediated expression in *N. benthamiana*. Tip6²²⁻²²⁶-mCherry, lacking a predicted signal peptide, localized in both, the nucleus and cytoplasm of *N. benthamiana* (Fig. 1c). To verify the localization of Tip6 in maize, we examined the expression of Tip6²²⁻²²⁶-mCherry in maize epidermal cells through biolistic bombardment. Confocal images showed

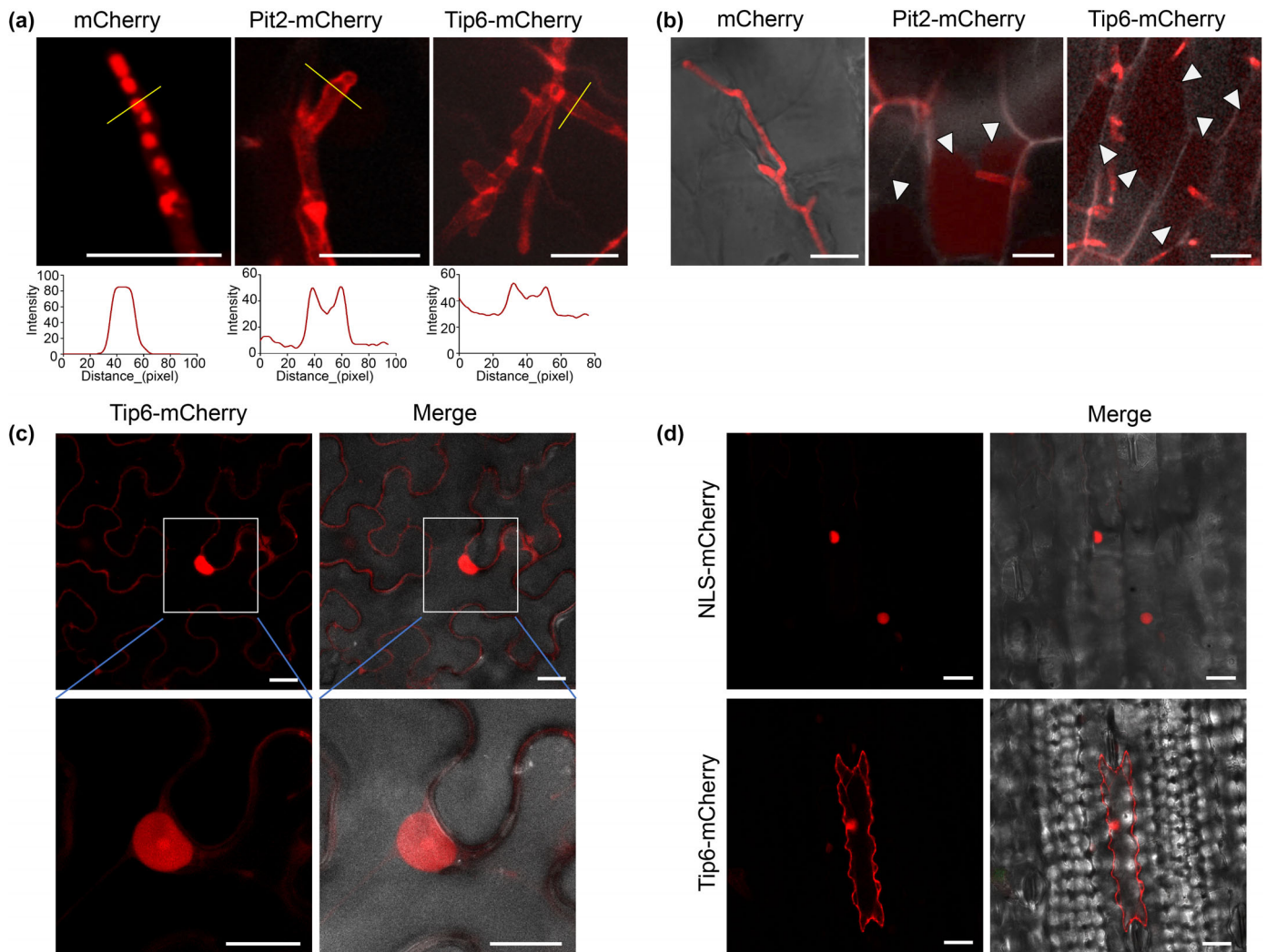


Fig. 1 Topless interacting protein 6 (Tip6) is a secreted and translocated into the host nucleus and cytoplasm during the *Ustilago maydis* infection. (a) Confocal laser scanning microscopy images showing the localization of Tip6 in *U. maydis* infection at 3 dpi postinfection. Fluorescent signals of *U. maydis* strains expressing SG200-*pPit2::mCherry*, SG200 Δ *pit2_pPit2::Pit2-mCherry*, or SG200 Δ *Tip6_pTip6::Tip6-mCherry* were visualized. SG200-*pPit2::mCherry* localized inside the hyphae, while SG200 Δ *pit2_pPit2::Pit2-mCherry* and SG200 Δ *Tip6_pTip6::Tip6-mCherry* mainly localized at the periphery of hyphae and hyphal tips. Fluorescence intensity profiles along the orange lines are displayed below the respective images. Bar, 20 μ m. (b) Secretion of Tip6 into the plant apoplast. Apoplastic spaces were enlarged by plasmolysis with 1 M NaCl. SG200-*pPit2::mCherry* did not diffuse into the apoplast, while the mCherry signals of SG200 Δ *pit2_pPit2::Pit2-mCherry* and SG200 Δ *Tip6_pTip6::Tip6-mCherry* diffused into the enlarged apoplast, as indicated by the arrows. Bar, 20 μ m. (c) Subcellular localization of Tip6 in *Nicotiana benthamiana* expressing *p2x35S::Tip6²²⁻²²⁶-mCherry*. White squares mark regions of interest, enlarged views of framed areas, revealing detailed subcellular localization. Images were observed at 2 dpi. Bar, 20 μ m. (d) Subcellular localization of Tip6 in maize epidermal cells expressing *p2x35S::NLS-mCherry* or *p2x35S::Tip6²²⁻²²⁶-mCherry*. NLS-mCherry served as a nuclear marker. Images were taken 16–24 h after transformation. Bar, 20 μ m.

that NLS-mCherry only localized in the maize nucleus, while Tip6²²⁻²²⁶-mCherry localized in both, the maize nucleus and cytoplasm (Fig. 1d). In conclusion, our results show that Tip6 is secreted and translocated into the host nucleus and cytoplasm during *U. maydis* infection.

Tip6 interacts with RELK2

To elucidate the function of Tip6, we performed a Co-IP assay followed by mass spectrometry analysis to identify its potential host targets. First, we expressed Tip6²²⁻²²⁶-GFP or GFP in *N. benthamiana* and conducted Co-IP (Fig. S1A; Table S2). Second, we infected maize seedlings with a Δ Tip6 strain expressing a

triple hemagglutinin (HA)-tagged Tip6 (SG200 Δ Tip6-*pPit2::Tip6-3xHA*) or a triple HA-tagged mCherry with signal peptide driven by the *Pit2* promoter (SG200-*pPit2::SP-mCherry-3xHA*), then performed immunoprecipitation (Fig. S1A,B; Table S3). Results from the mass spectrometry analysis are listed in Tables S2 and S3. Among the identified putative targets, the TOPLESS-RELATED 3 (NbTPR3) protein was one of the most significant in *N. benthamiana* samples. In maize samples, the maize TPL proteins RELK1, RELK2, REL2, and RELK3 were all identified as significant candidates. Additionally, maize Trps14 and bHLH40 transcription factors were identified. RELK2 was particularly noteworthy as it was only present in the Tip6 samples but absent in the controls (Fig. S1C; Table S3).

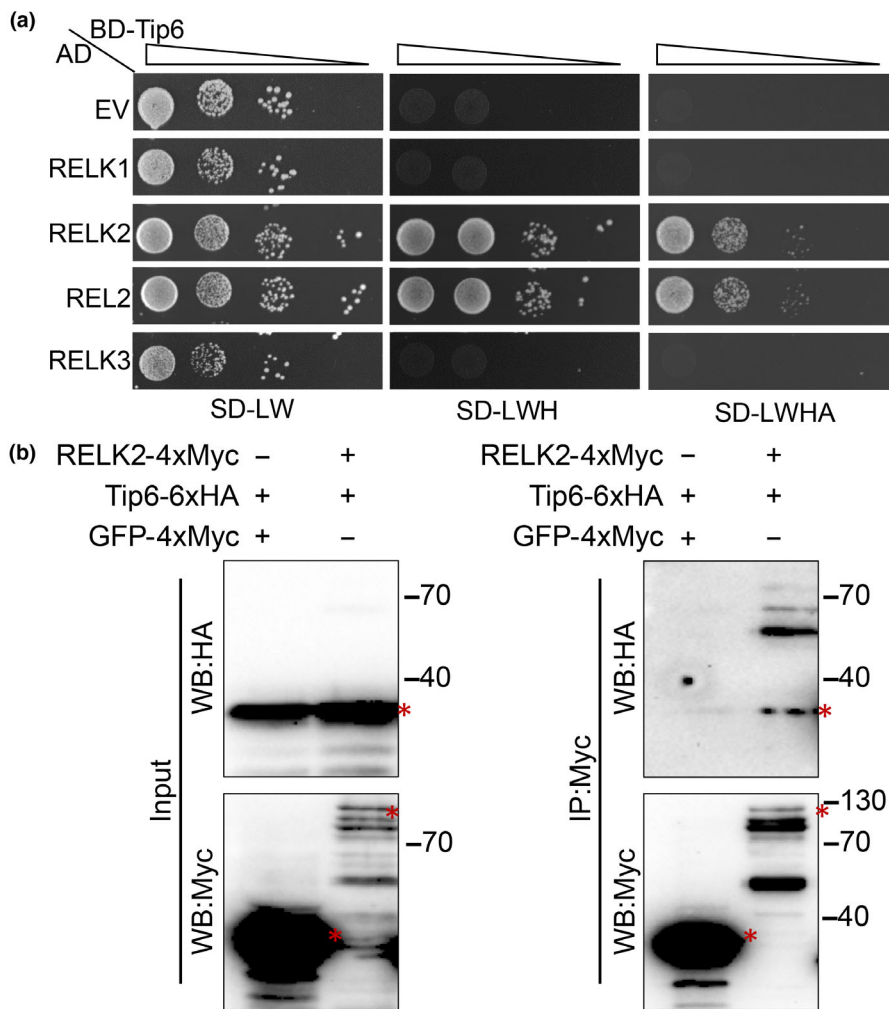


Fig. 2 Topless interacting protein 6 (Tip6) interacts with RELK2. (a) The interaction between Tip6 and maize TOPLESS (TPL) was assessed by yeast two-hybrid assay. Yeast cells co-transformed with designated plasmids were dropped in 10-fold serial dilutions on synthetic defined (SD) medium plates lacking essential amino acids, including leucine and tryptophan (SD-LW), histidine, leucine, and histidine (SD-LWH) or leucine, tryptophan, histidine, and adenine (SD-LWHA). Yeast cell growth on these plates was observed after 3–4 d. (b) Confirmation of Tip6 and RELK2 interaction by co-immunoprecipitation (Co-IP) assay in *Nicotiana benthamiana*. *N. benthamiana* plants were transiently co-expressed with p2x35S::Tip6²²⁻²²⁶-6xHA and either p2x35S::RELK2-4xMyc or p2x35S::GFP-4xMyc (as a control) for 2 d. Proteins were extracted and immunoprecipitated using magnetic Myc-trap beads. The presence of input and immunoprecipitated proteins (IP) was determined using anti-HA or anti-Myc antibodies, respectively. Expected bands are indicated by red asterisks.

To confirm the interaction between Tip6 and maize TPL family genes, we conducted a Y2H assay. The maize RELK1, RELK2, REL2, and RELK3 were each fused to GAL4AD, while Tip6²²⁻²²⁶ was genetically fused to GAL4BD. We attempted to test Trps14 and bHLH40 but encountered cloning difficulties. Our results revealed that Tip6 interacts with RELK2 and REL2, as shown by the growth on high-stringency selection media (Figs 2a, S2A). Conversely, no interaction was observed with RELK1 and RELK3 (Figs 2a, S2A), indicating that Tip6 selectively interacts with RELK2 and REL2. This suggests that Tip6 has a target specificity in maize TPL family proteins.

To emphasize the significance of RELK2, which was exclusively detected in the Tip6 samples while absent in the controls (Fig. S1C; Table S3), we conducted a co-IP assay in *N. benthamiana* to further validate the interaction between Tip6 and RELK2. The assay involved transient co-expression of Tip6²²⁻²²⁶-6xHA with RELK2-4xMyc, and as negative control, GFP-4xMyc was co-expressed with Tip6²²⁻²²⁶-6xHA. After *Agrobacterium* infiltration, proteins were extracted from *N. benthamiana* leaves and immunoprecipitated using α -Myc magnetic beads. The results revealed that Tip6²²⁻²²⁶-6xHA co-immunoprecipitated with

RELK2-4xMyc, whereas GFP-4xMyc did not (Fig. 2b), confirming the specific interaction between Tip6 and RELK2.

Tip6 specifically interacts with the N-terminal domain of RELK2

The TPL/TPR proteins have several highly conserved domains, with an N-terminal domain that consists of LisH, CTLH, and CRA domains, as well as a C-terminal domain consisting of two WD repeats (Ke *et al.*, 2015; H. Ma *et al.*, 2017; Martin-Arevalillo *et al.*, 2017). To elucidate, which domains of RELK2 are involved in interaction with Tip6, we conducted Y2H assays with various truncated forms of RELK2, such as the N-terminal domain (RELK2^N), C-terminal domain (RELK2^C), N-terminus lacking the CRA domain (RELK2^{NACRA}), and N-terminus CRA domain (RELK2^{CRA}; Fig. 3a). The results showed a strong interaction between the N-terminus of RELK2 and Tip6, indicating that RELK2^N is responsible for binding to Tip6, but not the WD40 repeat domain (Figs 3b, S2B,C).

To confirm the interaction between RELK2^N and Tip6, we performed Co-IP assays by co-expressing Tip6-4xMyc and RELK2^N-4xMyc or GFP-4xMyc in *N. benthamiana* leaves. This showed that

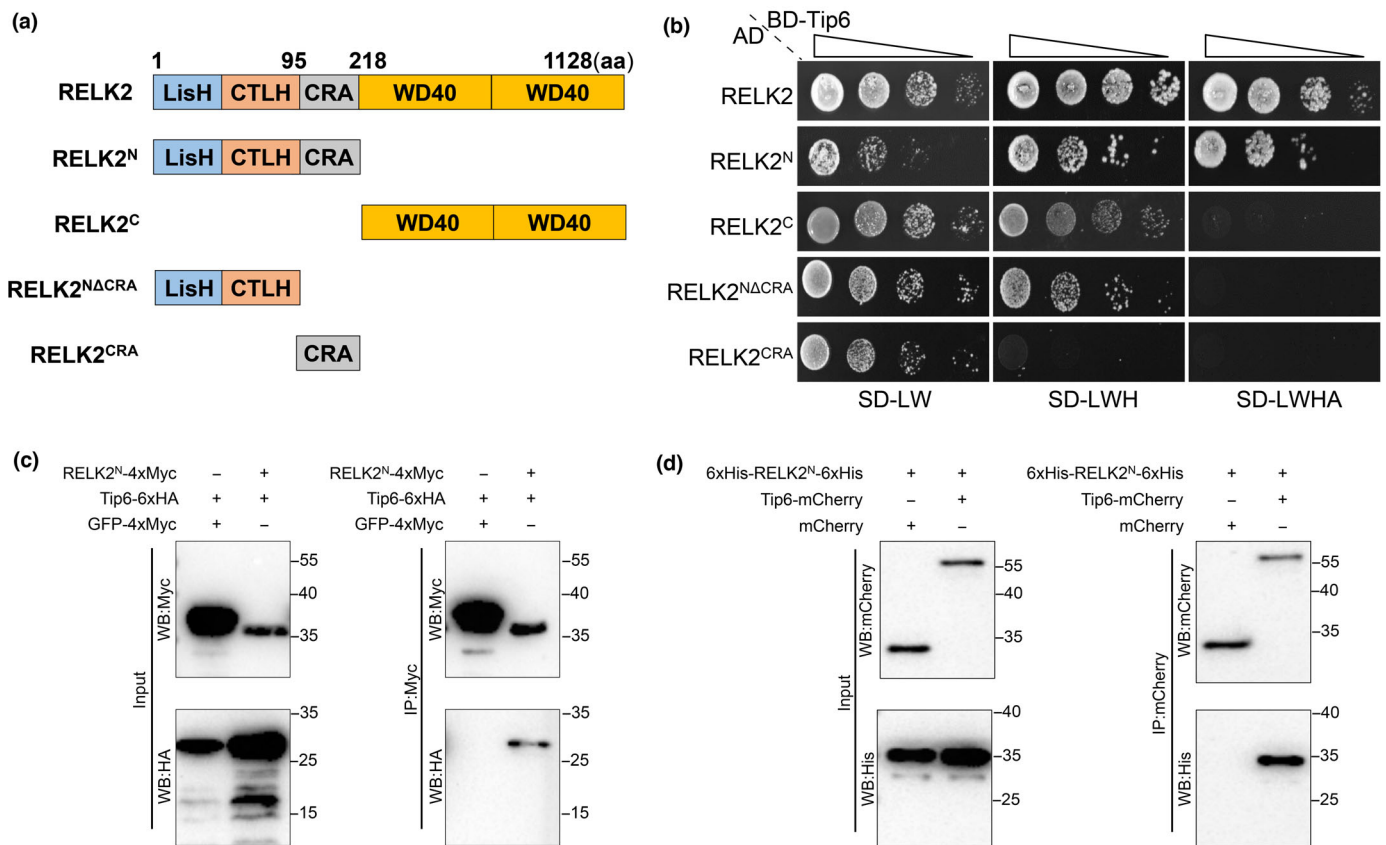


Fig. 3 Topless interacting protein 6 (Tip6) interacts with the N-terminus of RELK2. (a) Schematic representation of RELK2 and its truncated variants. The domain includes Lish (LIS1 homology domain), CTLH (C-terminal LisH motif domain), CRA (CT11-RanBPM domain), and the WD40 repeat domain. The variants include RELK2^N (1–218 aa of RELK2 N-terminal domain), RELK2^C (216–1128 aa of RELK2 C-terminal domain), RELK2^{NΔCRA} (1–95 aa of RELK2 N-terminus with Lish and CTLH domains), and RELK2^{CRA} (90–218 aa of RELK2 N-terminus, CRA domain). (b) Interaction between Tip6 and RELK2^N in the yeast two-hybrid assay. The plasmid carrying Tip6^{22–226} was co-transformed with plasmids carrying RELK2 truncated variants into yeast cells. Yeast cells were dropped in 10-fold serial dilutions on synthetic defined (SD) medium plates lacking essential amino acids, including leucine and tryptophan (SD-LW), histidine, leucine, and histidine (SD-LWH) or leucine, tryptophan, histidine, and adenine (SD-LWHA). (c) Tip6 interaction with the N-terminal domain of RELK2 was confirmed by a co-immunoprecipitation (Co-IP) assay. *Nicotiana benthamiana* plants were transiently co-expressed with p2x35S::Tip6^{22–226}-6xHA and either p2x35S::RELK2^N-4xMyc or p2x35S::GFP-4xMyc (control). Proteins were extracted and immunoprecipitated using magnetic Myc-trap beads. The presence of input and immunoprecipitated proteins (IP) was determined using anti-HA or anti-Myc antibodies, respectively. Full-length bands are indicated by red asterisks. (d) Tip6 interaction with the N-terminal domain of RELK2 was demonstrated in an *in vitro* pull-down assay. Recombinant His-RELK2^N-His protein was mixed with mCherry or Tip6-mCherry, and protein immunoprecipitation was performed using magnetic mCherry-trap beads. The immunoprecipitated proteins were detected using anti-His and anti-mCherry antibodies.

Tip6 was precipitated with RELK2^N-Myc, but not with GFP-4xMyc (Fig. 3c). Subsequently, we purified 6xHis-tagged RELK2^N using Ni-NTA agarose and GST-Tip6^{22–226}-mCherry and GST-mCherry using GST glutathione sepharose. We then removed the GST tag from Tip6^{22–226}-mCherry or mCherry using precission[®] protease and separated each protein using SEC. We collected and examined the proteins that migrated to the corresponding molecular masses (Fig. S3). The purified 6xHis-RELK2^N-6xHis and Tip6-mCherry or mCherry were subjected to an *in vitro* pull-down assay, which confirmed the interaction between RELK2^N and Tip6 (Fig. 3d). Together, these results indicate the importance of RELK2^N in the interaction with Tip6.

Tip6 EAR motifs mediate its binding to RELK2

The family of TPL/TPR proteins regulates gene expression in various biological processes through interactions with transcription

factors that possess repression domains (RDs), notably the EAR motif (PFAM: PF07897; Interpro: IPR012463; Masaru & Hideaki, 1995; Ohta *et al.*, 2001; Hiratsu *et al.*, 2003; Kagale & Rozwadowski, 2011; Causier *et al.*, 2012; Liu *et al.*, 2019). However, protein domain prediction using PFAM did not reveal any evidence of a RD in Tip6. Instead, we noticed the LxLxLx-type EAR motif with the similar sequences ‘LGLSLG’ and ‘TELSLGG’ in Tip6.

To investigate the function of those two potential EAR motifs, we generated deletion mutations for those two sequences and tested their interaction with RELK2 using Y2H assays (Fig. S4). The deletion mutation of ‘LGLSLG’ showed reduced interaction with RELK2, while the deletion mutation of ‘TELSLGG’ resulted in a loss of interaction with RELK2, indicating that both motifs function as EAR motifs with an impact on Tip6’s interaction with RELK2 (Fig. S4).

Moreover, we generated point mutations in those two sequences and tested their interaction with RELK2 using Y2H

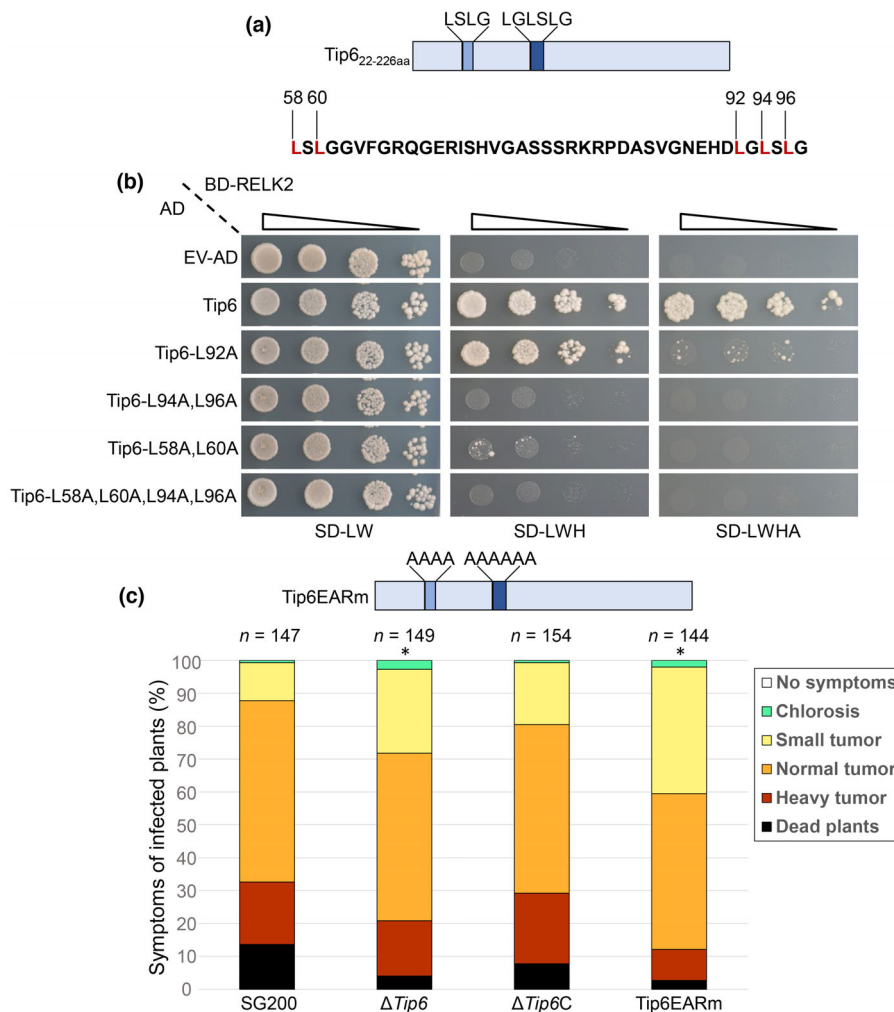


Fig. 4 Ethylene-responsive element binding factor-associated amphiphilic repression (EAR) motifs of Topless interacting protein 6 (Tip6) are essential for interaction with RELK2 and virulence activity. (a) Schematic representation of Tip6 EAR motifs. Tip6 contains two EAR repression domains, and the numbers above the protein sequence indicate the positions of the point mutations of the EAR motifs. (b) Yeast two-hybrid assay to assess interactions between Tip6 EAR motif variants and RELK2. (c) Virulence activity of the Tip6 deletion mutant (Δ Tip6), its full-length complementation (Δ Tip6C), and its EAR motifs mutant version (Tip6EARm). The protein sequence in the figure represents the mutated positions of the EAR motifs, which have been substituted with alanine. Maize seedlings (7 d old) were infected with *Ustilago maydis* strains, and disease symptoms were scored at 12 dpi. Asterisks indicate significant differences ($P < 0.05$; Student's *t*-test). The experiments were repeated three times.

assays (Fig. 4a). Our results showed that full-length Tip6 interacted with RELK2, consistent with our previous findings. However, Tip6_L92A displayed a reduction in binding to RELK2 (Fig. 4b). Conversely, Tip6_L94A, L96A failed to interact with RELK2, as shown by almost no growth on the selection medium (Fig. 4b). This suggests that leucine residues at positions 94 and 96 within the 'LGLSLG' motif are more crucial for the Tip6-RELK2 interaction.

We also conducted a Y2H assay with RELK2 to assess the binding capability of Tip6_L58A, L60A mutants of the 'TELSLGG' sequence (Fig. 4a). Our results showed that Tip6_L58A, L60A exhibited insufficient growth on intermediate stringency medium and almost no growth on high-stringency medium (Fig. 4b). This finding confirms that the 'TELSLGG' sequence in Tip6 functions as an EAR motif, and it is crucial for Tip6 to bind to RELK2.

To assess the impact of both EAR motifs, we generated mutants with deletions in both motifs and the Tip6_L58A, L60A, L94A, and L96A (Tip6_Quad) mutants and tested their ability to bind RELK2 (Figs 4a, S4). This revealed that both the Tip6 two EAR motif deletion mutant and Tip6_Quad completely lost their interaction with RELK2, as reflected by no growth

on the plates (Figs 4b, S4). These findings suggest that both EAR motifs within Tip6 are critical for its interaction with RELK2. Therefore, we propose that Tip6 interacts with RELK2 partially through these two LxLxLx-type EAR motifs.

We further checked the conservation of Tip6 across various smut species through an ortholog search, revealing only two orthologs, notwithstanding their relatively low sequence identity. Interestingly, despite this divergence, the essential EAR motifs within Tip6 are conserved across its two ortholog genes (Fig. S5A). Furthermore, previous experimental evidence has indicated that despite its sequence diversity, *Sporisorium reilianum* SrTip6, which shares only 25.65% identity with UmTip6, can effectively substitute for UmTip6 without compromising virulence in *U. maydis* (Zuo *et al.*, 2021). To investigate the functional conservation of SrTip6, we conducted Y2H assays to assess the interaction between SrTip6 and maize TPL family proteins. The results showed that SrTip6 interacts with REL2 and RELK2, mirroring the interaction pattern observed for UmTip6 (Fig. S5B). This conservation in interaction partners may imply the functional importance of these motifs in facilitating effective interactions during plant-pathogen interactions.

To assess the functional significance of the EAR motifs identified in Tip6, we conducted experiments to investigate their impact on the virulence of *U. maydis*. Specifically, we complemented a CRISPR/Cas9-generated Tip6 frameshift SG200 mutant with either the full-length Tip6 or an EAR mutant (Tip6EARm), in which the EAR motif sequences 'LGLSLG' and 'LSLG' were replaced with sequential alanine. Complementation with full-length Tip6 restored the virulence of Δ Tip6 to a level similar to that of SG200. However, the Tip6EARm mutant could not restore the lost virulence and even exhibited a significant reduction in virulence compared with SG200 (Fig. 4c). These findings strongly suggest that the identified EAR motifs, including the 'LGLSLG' motif and the 'LSLG' motif in Tip6 are crucial for the full virulence of *U. maydis*.

Tip6 interferes with nuclear aggregation of RELK2

To determine the subcellular localization of RELK2, we transiently overexpressed RELK2-GFP in *N. benthamiana* plants. Confocal imaging revealed that RELK2-GFP accumulated in the nucleus and formed speckles (Fig. S6A). Further investigation of RELK2-GFP overexpression in maize epidermal cells showed a similar nuclear localization pattern to that observed in *N. benthamiana*, confirming the nuclear localization of RELK2-GFP (Fig. S6B). We also checked the localization of RELK1-GFP and REL2-GFP under overexpression. They are localized in the nucleus, but do not form nuclear speckles (Fig. S7A).

To ascertain the effect of Tip6 on the subcellular localization of RELK2, we co-overexpressed RELK2-GFP with either Tip6-mCherry or mCherry in *N. benthamiana*. Remarkably, this showed that the presence of Tip6 resulted in a significant decrease in the number of nuclear speckles of RELK2-GFP, whereas the speckle pattern remained unchanged in the presence of mCherry (Fig. 5a). Additionally, it is worth noting that some fraction of RELK2 is also localized in the cytoplasmic compartment (Fig. 5a). Moreover, we assessed the co-overexpression of Tip6 with either RELK1-GFP or REL2-GFP, and observed no changes in the nuclear signaling of RELK1-GFP or REL2-GFP (Fig. S7B).

As mentioned previously, the EAR motifs of Tip6 play a crucial role in binding to RELK2 (Figs 4b, S4). To examine the role of the EAR motifs in Tip6 in altering the localization of RELK2, we co-overexpressed RELK2-GFP with a Tip6 Δ EARs-mCherry mutant lacking the EAR motifs in *N. benthamiana*. Surprisingly, confocal imaging revealed that the Tip6 mutant was unable to alter the nuclear distribution pattern of RELK2, as seen by the RELK2-GFP localized to nuclear speckles, similar to the case with mCherry co-expression (Fig. 5a). Moreover, we found that Tip6 Δ EARs cannot interact with RELK2 via the Y2H assay (Fig. S4B). To further validate the role of Tip6 in altering the nuclear speckle formation of RELK2, we quantified the number of speckles in *N. benthamiana* co-overexpressing cells. This showed that the number of RELK2 speckles significantly decreased in cells co-expressing Tip6 compared with cells expressing mCherry. However, when we co-overexpressed Tip6 Δ EARs mutant, the number of RELK2 speckles was similar to that of mCherry (Fig. 5b).

To investigate the impact of Tip6 on RELK2 in maize, we transiently co-overexpressed RELK2-GFP along with either Tip6-mCherry or mCherry alone in maize epidermal cells. Confocal imaging revealed that co-expression with mCherry led to the localization of RELK2-GFP in nuclear speckles. Conversely, when co-expressed with Tip6-mCherry, these speckles are notably reduced or nearly absent (Fig. 5c). In summary, while the influence of Tip6 on RELK2's nuclear localization at endogenous levels remains unknown, our results demonstrate that Tip6 significantly modulates the nuclear distribution pattern of RELK2 during overexpression, with the EAR motifs of Tip6 playing crucial in this process.

Tip6 interferes with RELK2-regulated transcription factors

To gain insights into the mechanisms underlying Tip6 virulence and assess the impact of its EAR motifs on infection, we performed transcriptome RNA-sequencing (RNA-Seq) analysis on maize seedling leaves infected with SG200, Δ Tip6, or Tip6EARm at 3 dpi. Using a threshold of absolute \log_2 Foldchange > 1 and *P*-value < 0.05, we found that compared with maize infected with SG200, Δ Tip6 had 91 upregulated and 71 downregulated DEGs, while Tip6EARm displayed 191 upregulated and 115 downregulated DEGs (Fig. S8A,B; Datasets S5, S6).

To examine the biological pathways associated with the DEGs, we performed a GO enrichment analysis. The GO analysis of DEGs between Δ Tip6 and SG200 revealed the regulation genes related to 'cellular biosynthetic', 'transcription', 'gene expression', and 'RNA metabolic' processes (Fig. S8C; Datasets S7). Particularly, the majority of the regulated genes were involved in transcriptional regulation. Among the 18 transcription factors DEGs, nine belonged to the AP2/ERF family, with seven upregulated genes belonging to the ERF B1 family (Fig. 6a; Dataset S8). The remaining two downregulated genes were classified as members of the AP2 and DREB families, respectively. Among these DEGs, we observed the downregulation of *Branched silkless 1 (bd1)*, a gene known to regulate inflorescence formation from spikelet formation in maize (Chuck *et al.*, 2002). Additionally, we found that the maize genes *dbp4* (ZmDBP4) and *CBF3* were upregulated, which were highly activated by cold and play regulatory roles in the abiotic stress responses of plants (Wang *et al.*, 2011; Han *et al.*, 2020). The downregulated *ereb26*, a member of the AP2 subfamily, is known to be highly involved in floral formation (Kunst *et al.*, 1989).

Several of the identified genes in the comparison of Δ Tip6 and SG200 have known orthologs in other species. For instance, ovate transcription factors have been shown to be repressor regulators in *Arabidopsis* ovate family protein 1 (AtOFP1), which inhibits cell elongation, and rice ovate family protein 6 (OsOFP6), which regulates lateral root growth, leaf inclination, and responses to abiotic stimuli (Wang *et al.*, 2007; Y. Ma *et al.*, 2017; Sun *et al.*, 2020). SHI/STY transcription factors are involved in organ development and hormone regulation (Zhang *et al.*, 2015; He *et al.*, 2019; Fang *et al.*, 2023). The *Arabidopsis* homolog of ZmNAC73, Junghunnen1 (JUB1), acts as a negative regulator of leaf senescence (Wu *et al.*, 2012). Additionally,

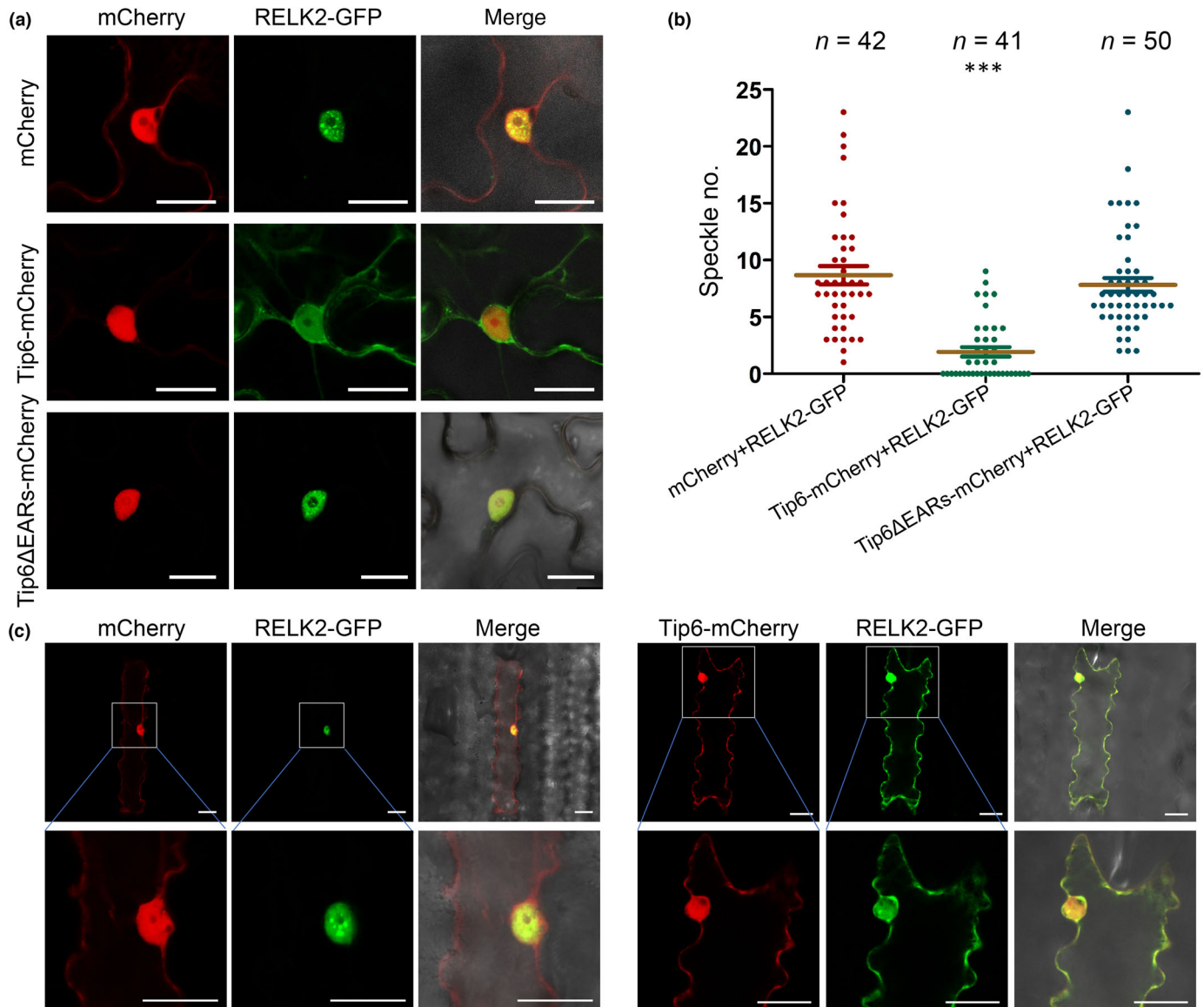


Fig. 5 Effects of Topless interacting protein 6 (Tip6) on the nuclear distribution pattern of RELK2 through its ethylene-responsive element binding factor-associated amphiphilic repression (EAR) motifs. (a) Confocal microscopy images showing the nuclear distribution pattern of RELK2 in the presence of mCherry, Tip6²²⁻²²⁶-mCherry, or Tip6²²⁻²²⁶ΔEARs-mCherry (with deleted EAR motifs). *Nicotiana benthamiana* epidermal cells were co-expressed with p2x35S::RELK2-GFP and either p2x35S::mCherry, p2x35S::Tip6²²⁻²²⁶-mCherry, or p2x35S::Tip6²²⁻²²⁶ΔEARs-mCherry. Bar, 20 μm. (b) Comparison of the number of RELK2 nuclear speckles in the presence of mCherry, Tip6²²⁻²²⁶-mCherry or Tip6²²⁻²²⁶ΔEARs-mCherry. The number of RELK2 nuclear speckles was counted in the cells shown in (a). Results were obtained from three independent experiments. N represents the total number of nuclei ($P < 0.001$, ANOVA, Tukeys). (c) Confocal microscopy images depict the nuclear distribution pattern of RELK2 in the presence of mCherry or Tip6²²⁻²²⁶-mCherry. *Zea mays* epidermal cells were co-expressed with p2x35S::RELK2-GFP along with either p2x35S::mCherry or p2x35S::Tip6²²⁻²²⁶-mCherry constructs. The images were captured at 24 h postinfection (hpi). Bar, 20 μm.

we observed the upregulation of *wrky80*, which belongs to a family of transcription factors known to play crucial roles in disease resistance and response to abiotic stress (Rushton *et al.*, 2010; Hu *et al.*, 2021). Overall, Tip6-responsive maize genes are involved in various biological processes, including meristem maintenance, floral organ morphogenesis, disease resistance, and abiotic stress response.

The GO analysis of DEGs between Tip6EARm and SG200 showed the regulation of genes associated with ‘cellular

biosynthetic’, ‘transcription’, ‘gene expression’, and ‘RNA metabolic’ processes (Fig. S8D; Dataset S9). Among the 48 differentially expressed transcription factors, 20 belonged to the AP2/ERF family (Fig. 6b; Dataset S10). Interestingly, 19 of these AP2/ERF family members were upregulated, while *bd1* showed downregulation, as seen in Δ*Tip6*-infected maize. Additionally, the comparison of DEGs between Δ*Tip6* and SG200, as well as between Tip6EARm and SG200, revealed that nine DEGs exhibited similar regulation, with seven of them belonging to the AP2/ERF

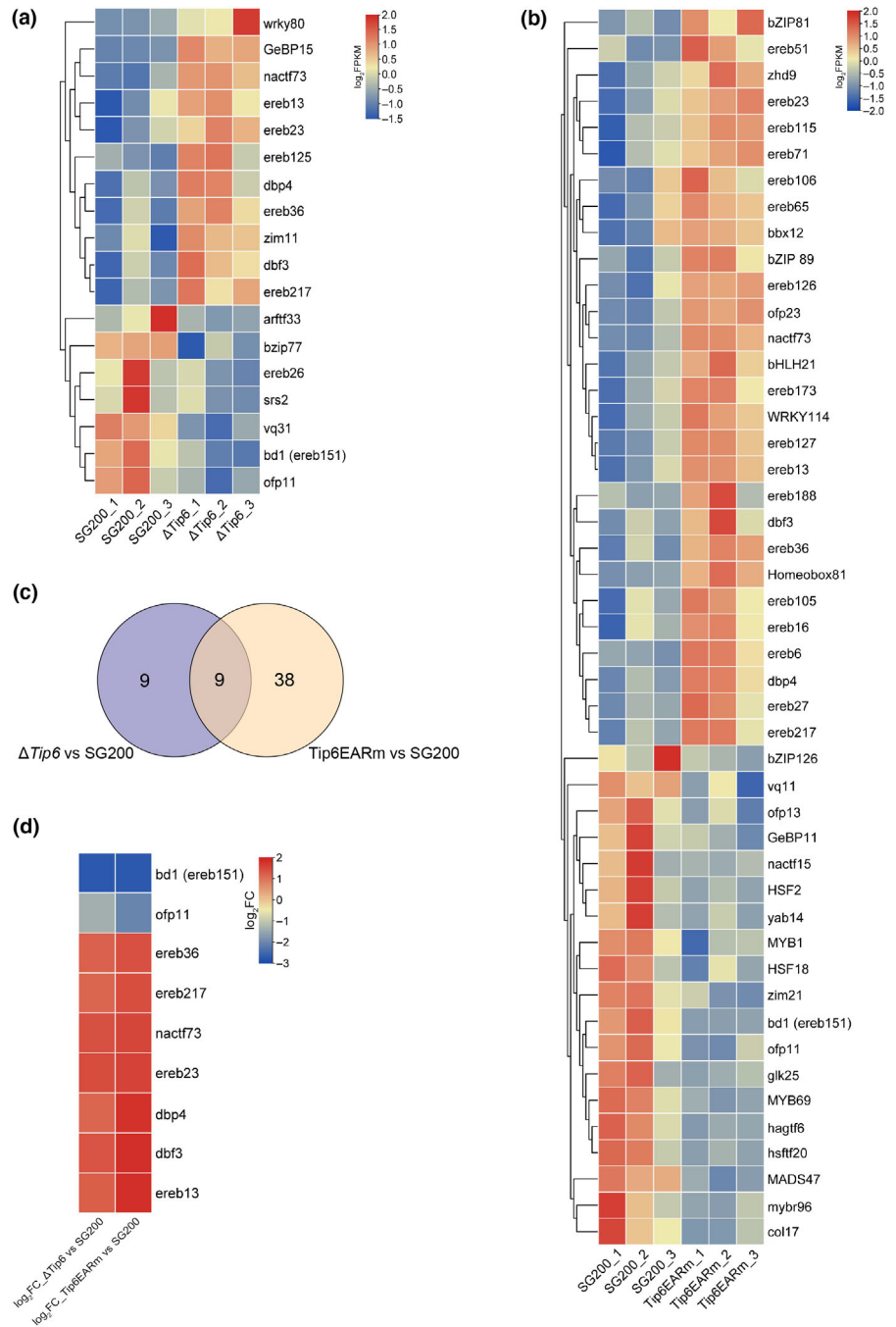


Fig. 6 Impact of Topless interacting protein 6 (Tip6) on host transcription factors' expression. (a) Heatmap illustrating the differential expression genes (DEGs) in maize infected with $\Delta Tip6$ and SG200 strains. The \log_2 FPKM values, based on the original FPKM values, were used to construct the heatmap. Rows and columns were created using the Euclidean distance method and the complete linkage method via TBTOOLS (Chen *et al.*, 2020). Gene expression is displayed on a red-to-blue spectrum, with red indicating high expression and blue indicating low expression. (b) Heatmap of DEGs in maize infected with Tip6EARM and SG200 strains. (c) Venn diagram depicting the shared DEGs in $\Delta Tip6$ and Tip6EARM compared with SG200 samples. (d) Heatmap showing the shared DEGs in $\Delta Tip6$ vs SG200 and Tip6EARM vs SG200. The \log_2 fold change in expression of $\Delta Tip6$ and Tip6EARM compared with SG200 is depicted.

family (Fig. 6c,d). These findings suggest that Tip6 may suppress a specific group of host transcription factors, particularly those in the AP2/ERF family, suggesting its regulatory role in the transcriptional modulation of the host plant.

We therefore hypothesized that the interaction between Tip6 and RELK2 affects the recruitment of host transcription factors and subsequent host gene expression. However, we did not find any differentially expressed maize TPL genes in our RNA-Seq data. To identify potential regulators of the DEGs, we performed an enrichment analysis using the PLANTTFDB database

(<http://planttfdb.cbi.pku.edu.cn>) (Jin *et al.*, 2017; Tian *et al.*, 2020). In the comparison of $\Delta Tip6$ vs SG200 DEGs, we observed enrichment of 11 transcription factors ($P < 0.05$; Fig. S9A; Dataset S11). Notably, *ereb125* exhibited upregulation and putative regulation of 31 DEGs (Fig. S9A). Furthermore, *ereb125* was implicated in the putative regulation of other upregulated transcription factors, including *dbp4*, *zim11*, *NACT73*, and *wrky80* (Dataset S12).

Similarly, in the comparison of Tip6EARM vs SG200 DEGs, we observed enrichment of 31 transcription factors (Fig. S9B;

Dataset S13), including REL2 interactors *ramosa2* and *ereb147* (Liu *et al.*, 2019). Moreover, *ereb125* was found to putatively regulate 61 DEGs, including *dbp4*, *NAC73*, *ereb51*, *hb81*, *bHLH21*, and *ereb127* (Fig. S9B; Datasets S13, S14). These findings strongly suggest that Tip6 plays a significant role in the regulation of host transcription factors, particularly those belonging to the AP2/ERF family.

Discussion

In this study, we demonstrate that the *U. maydis* effector Tip6 promotes tumorigenesis by targeting maize RELK2 through its EAR motifs. Tip6 mimics the plant recruitment mechanism, disrupting host gene expression by recruiting the N-terminal domain of RELK2 via its EAR domains. Mutation of the leucine residue in the EAR motifs abolishes the interaction of Tip6 with RELK2. Moreover, Tip6EARm fails to restore the defective virulence phenotype of Δ Tip6. Interestingly, the *U. maydis* effector Nkd1 also interacts with RELK2 via an EAR motif, but deletion or mutation of the EAR motif in Nkd1 reduces the interaction without affecting its ability to complement Δ Nkd1-deficient virulence, unlike Tip6 (Navarrete *et al.*, 2022).

Tip6 binding to RELK2 is diminished upon mutation or deletion of either of the EAR motifs (sequence with TELSLG or LGLSLG), indicating the importance of having two EAR motifs for enhanced binding capacity. While the 'LGLSLG' sequence conforms to the typical EAR motif sequence type, 'LSLG' does not. However, we identified 'TELSLG' as an EAR motif due to its impact on the interaction with RELK2. This observation aligns with computational predictions made by modeling the Tip6-RELK2 N-terminal binding using AlphaFold, which suggested that 'TELSL' is a critical binding position (Khan *et al.*, 2023).

This finding raises the question of why Tip6 possesses two EAR motifs. To shed light on this, we can draw a parallel with the Aux/IAA repressor 7 (IAA7) in *Arabidopsis*, which also has two EAR motifs with different roles. In AtIAA7, the second EAR motif plays a minor role in repression but is crucial for interaction with TPR1, whereas the first EAR motif plays a major role in both repression and interaction with all TPL/TPR members (Lee *et al.*, 2016). This suggests that the presence of two EAR motifs in Aux/IAA repressors provides greater repression capacity and interaction diversity compared with those with a single EAR motif (Lee *et al.*, 2016).

Similarly, the recently discovered rhizogenic *Agrobacterium* protein RolB has an N- and a C-terminal EAR motif, but only the C-terminal EAR motif is required for TPL recruitment and hairy root development (Gryffroy *et al.*, 2023). Drawing from these examples, we can speculate that the presence of two EAR motifs in Tip6 may confer similar functional advantages. While the exact mechanism and significance of this enhanced binding capacity in Tip6 remain unclear, our findings demonstrate that Tip6EARm, similar to the Nkd1SRDX mutants with increased binding capacity to TPL, results in a significant loss of virulence. These findings highlight the critical role of the precise binding strengths exhibited by Tip6 or Nkd1 to RELK2 in their pathogenic role in *U. maydis*.

Our RNA-Seq analysis identified 57 differentially expressed maize transcription factors in the presence of Tip6. Among the 22 AP2/ERF DEGs, 20 were downregulated, with 13 belonging to the B1 family and 2 being upregulated. Jsi1 and RolB activate the ERF B3 branch of the JA/ET signaling pathway by recruiting TPL (Darino *et al.*, 2020; Gryffroy *et al.*, 2023). The ERF B3 subfamily acts as a positive transcriptional regulator, activating defense-related genes in the JA/ET hormone signaling pathways. Interestingly, we did not find any B3 group genes among our data, and GO analysis of Tip6-regulated DEGs shows that they are not enriched in the JA/ET pathway, which is in line with different ERF branches being affected. Three pairs of paralogs were found in the B1 branch genes of DEGs: *dbf3/ereb36*, *ereb105/ereb16*, and *ereb13/ereb217* (Cheng *et al.*, 2023). Therefore, we propose that the ERF branch affected by Tip6 is more closely related to plant growth and development, influencing leaf tumor formation by *U. maydis*.

Our study highlights *ereb125* as a potential regulator of a significant number of DEGs. Although the exact function of *ereb125* in maize is yet to be determined, its ortholog in *Arabidopsis*, *LEAFY PETIOLE (LPE; AT5G13910.1)* was initially discovered in mutant screens for leaf development (van der Graaff *et al.*, 2000). In wild-type *Arabidopsis*, the expression of the *LPE* gene is very low and strongest in young leaves, with weaker expression in older leaves, suggesting tissue-specific roles (van der Graaff *et al.*, 2000). These findings suggest a potential role for *ereb125* in leaf development. Therefore, we hypothesize that the interaction between Tip6 and RELK2 may involve *ereb125*, thus promoting leaf tumor formation.

U. maydis effector genes display highly distinct stage-specific expression patterns during maize infection, suggesting potential differences in their functions and host adaptation (Lanver *et al.*, 2018). Among these effectors, Tip6 and Tip7 show peak expression at 2 dpi during early biotrophic development, while Jsi1 peaks at 4 dpi, Nkd1 at 6–8 dpi, and Tip8 at 8 dpi, coinciding with tumor formation (Darino *et al.*, 2020; Navarrete *et al.*, 2022; Khan *et al.*, 2023). By contrast, Tip1–Tip5, except for Tip3, which peaks at 4 dpi, all exhibit peak expression at 2 dpi (Bindics *et al.*, 2022). This time-staggered expression pattern suggests a potential strategy employed by the pathogen to avoid competitive recruitment of the corepressor TPL at different infection stages. Additionally, it implies functional variations among these effectors in modulating host responses. Notably, these effectors employ different mechanisms to target maize TPL proteins, resulting in pleiotropic effects. Jsi1, Nkd1, Tip6, and Tip7 recruit TPL through RDs (LxLxLx or DLNxxP), while Tip1–Tip5 and Tip8 engage TPL through a RD-independent mechanism. Interestingly, despite their potential functional redundancy, individual knockouts of Tip6 and Nkd1 resulted in virulence deficiencies, indicating their unique roles during infection. However, the simultaneous deletion of multiple effectors led to a more pronounced virulence deficiency, highlighting the collective impact of these proteins on manipulating host responses (Bindics *et al.*, 2022; Khan *et al.*, 2023). It is worth noting that the maize RELK2 protein-interacting partners are located on different chromosomes, which may suggest a strategic evolution of

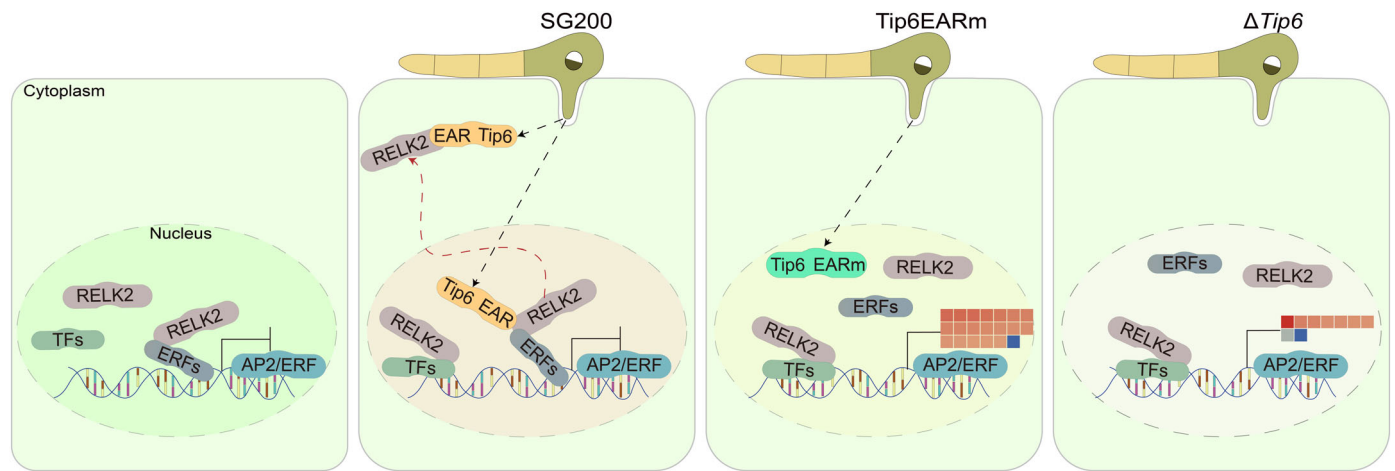


Fig. 7 Topless interacting protein 6 (Tip6) impacts host gene regulation by interacting with the RELK2 corepressor. The healthy plant cell where ERF family transcription factors recruit RELK2 and repress AP2/ERF family transcription factors. While some unknown transcription factors (TFs) present, they do not recruit RELK2 yet. SG200 strain infected cell, where Tip6 is expressed and secreted into the plant host. Tip6 interacts with RELK2 utilizing ethylene-responsive element binding factor-associated amphiphilic repression (EAR) repressive motifs, leading to a change in the localization of RELK2 from the nucleus to the cytoplasm and interfering with its repressor proteins. Tip6 with the EAR motif mutated into alanine, which loses the ability to interact with RELK2. This loss of interaction causes an unknown impact that leads to the mis-regulation of AP2/ERF family transcription factors. The knockout mutant, which lacks Tip6 and its interaction with RELK2, suggests that Tip6 plays a crucial role in the pathogenesis of *Ustilago maydis*.

effector-host interactions to target multiple TPL proteins effectively (Khan *et al.*, 2023).

Furthermore, Jsi1, Nkd1, and Tip1–Tip5 activate genes involved in hormone signaling pathways, including JA/ET, auxin, and SA, by relieving TPL-mediated repression and promoting plant defense responses, thereby ultimately increasing susceptibility to *U. maydis* infection (Darino *et al.*, 2020; Bindics *et al.*, 2022; Navarrete *et al.*, 2022). By contrast, our finding regarding Tip6 did not reveal a clear correlation with hormone pathways. Although we identified several DEGs related to hormones, Tip6 did not appear to significantly enrich these pathways. Instead, our data suggest that Tip6 may influence plant development during leaf tumor formation by interfering with RELK2. Additionally, overexpression of Tip6 in *N. benthamiana* found an auxin signaling-inducing capacity in the plant (Khan *et al.*, 2023).

These findings suggest the diverse strategies employed by *U. maydis* effectors to target and impact maize TPL activity, emphasizing the critical role of TPL as a central hub of plant transcriptional regulation during *U. maydis* invasion. Similar mechanisms have been observed in other species, such as the oomycete *Hyaloperonospora arabidopsidis* (Hpa) effector HaRxL21 and the rhizogenic *Agrobacterium* protein RolB, both of which interact with TPL through their EAR motifs to regulate host genes (Harvey *et al.*, 2020; Gryffroy *et al.*, 2023).

Our study demonstrates that Tip6 recruits the N-terminus of RELK2 through its two EAR motifs. This changes the formation of nuclear speckles under overexpression and interferes with the dysregulation of many host transcription factors. Notably, we observed a downregulation of ERF B1 branch genes associated with host development. In conclusion, we propose a simplified working model illustrating the interference of Tip6 with RELK2 (Fig. 7). We hypothesize that this mechanism may directly

contribute to the specific virulence of Tip6 in leaf tumor formation. Our study sheds light on the function of Tip6 through protein interactome and gene transcriptome analysis. Future studies will aim to fully comprehend the molecular mechanisms by which Tip6 manipulates RELK2 and influences leaf tumor formation.

Acknowledgements

We express our gratitude to Anne Harzen for her valuable assistance in MS sample processing, and to Shan Gao for his expertise in mapping the raw RNA-Seq data to count files. We acknowledge the funding received from the European Research Council (ERC) under the European Union’s Horizon 2020 research and innovation program (grant agreement no 771035), as well as the support from the Deutsche Forschungsgemeinschaft (DFG, German Research Foundation) under Germany’s Excellence Strategy – EXC-2048/1 – Project ID: 390686111. We also acknowledge the financial support provided by the China Scholarship Council (Grant no. 201806320134). Open Access funding enabled and organized by Projekt DEAL.


Competing interests

None declared.

Author contributions

GD, LH and BÖ designed the research. LH, BÖ, M Kastl, M Khan, DH and AD conducted the experiments. LH performed the RNA-Seq data differential gene analysis. SCS and HN carried out the MS and MS data analysis. LH and GD wrote the paper with contributions from the other authors.

ORCID

Armin Djamei  <https://orcid.org/0000-0002-8087-9566>
 Gunther Doehlemann  <https://orcid.org/0000-0002-7353-8456>
 Hirofumi Nakagami  <https://orcid.org/0000-0003-2569-7062>

Data availability

The RNA-Seq raw data are publicly accessible in the NCBI Gene Expression Omnibus under accession no. GSE234067. The mass spectrometry proteomics data are available in the ProteomeX-change Consortium via the PRIDE (Perez-Riverol *et al.*, 2022) partner repository with the dataset identifier PXD042605.

References

- Bellande K, Trinh D, Gonzalez A, Dubois E, Petitot A, Lucas M, Champion A, Gantet P, Laplace L, Guyomarc'h S. 2022. PUCHI represses early meristem formation in developing lateral roots of *Arabidopsis thaliana*. *Journal of Experimental Botany* 73: 3496–3510.
- Bindics J, Khan M, Uhse S, Kogelmann B, Baggely L, Reumann D, Ingole KD, Stürnberg A, Rybecky A, Darino M *et al.* 2022. Many ways to TOPLESS – manipulation of plant auxin signalling by a cluster of fungal effectors. *New Phytologist* 236: 1455–1470.
- Büttner M, Singh KB. 1997. *Arabidopsis thaliana* ethylene-responsive element binding protein (AtEBP), an ethylene-inducible, GCC box DNA-binding protein interacts with an ocs element binding protein. *Proceedings of the National Academy of Sciences, USA* 94: 5961–5966.
- Causier B, Ashworth M, Guo W, Davies B. 2012. The TOPLESS interactome: a framework for gene repression in Arabidopsis. *Plant Physiology* 158: 423–438.
- Chakravarthy S, Tuori RP, D'Ascenzo MD, Fobert PR, Despres C, Martin GB. 2003. The tomato transcription factor Pti4 regulates defense-related gene expression via GCC box and non-GCC box cis elements. *Plant Cell* 15: 3033–3050.
- Chandler JW. 2018. Class VIIIb APETALA2 ethylene response factors in plant development. *Trends in Plant Science* 23: 151–162.
- Chen C, Chen H, Zhang Y, Thomas HR, Frank MH, He Y, Xia R. 2020. TBTOOLS: an integrative toolkit developed for interactive analyses of big biological data. *Molecular Plant* 13: 1194–1202.
- Cheng C, An L, Li F, Ahmad W, Aslam M, Ul Haq MZ, Yan Y, Ahmad RM. 2023. Wide-range portrayal of AP2/ERF transcription factor family in maize (*Zea mays* L.) development and stress responses. *Genes* 14: 1.
- Chuck G, Muszynski M, Kellogg E, Hake S, Schmidt RJ. 2002. The control of spikelet meristem identity by the branched silkless1 gene in maize. *Science* 298: 1238–1241.
- Cox J, Mann M. 2008. MAXQUANT enables high peptide identification rates, individualized p.p.b.-range mass accuracies and proteome-wide protein quantification. *Nature Biotechnology* 26: 1367–1372.
- Darino M, Chia KS, Marques J, Aleksza D, Soto-Jiménez LM, Saado I, Uhse S, Borg M, Betz R, Bindics J *et al.* 2020. *Ustilago maydis* effector Jsi1 interacts with Topless corepressor, hijacking plant jasmonate/ethylene signaling. *New Phytologist* 229: 3393–3407.
- Djamei A, Schipper K, Rabe F, Ghosh A, Vincon V, Kahnt J, Osorio S, Tohge T, Fernie AR, Feussner I *et al.* 2011. Metabolic priming by a secreted fungal effector. *Nature* 478: 395–398.
- Dobin A, Davis CA, Schlesinger F, Drenkow J, Zaleski C, Jha S, Batut P, Chaisson M, Gingeras TR. 2013. STAR: ultrafast universal RNA-seq aligner. *Bioinformatics* 29: 15–21.
- Fang D, Zhang W, Ye Z, Hu F, Cheng X, Cao J. 2023. The plant specific SHORT INTERNODES/STYLISH (SHI/STY) proteins: structure and functions. *Plant Physiology and Biochemistry* 194: 685–695.
- Fujimoto SY, Ohta M, Usui A, Shinshi H, Ohme-Takagi M. 2000. Arabidopsis ethylene-responsive element binding factors act as transcriptional activators or repressors of GCC box-mediated gene expression. *Plant Cell* 12: 393–405.
- Gallavotti A, Long JA, Stanfield S, Yang X, Jackson D, Vollbrecht E, Schmidt RJ. 2010. The control of axillary meristem fate in the maize ramosa pathway. *Development* 137: 2849–2856.
- Ge SX, Jung D, Yao R. 2020. SHINYGO: a graphical gene-set enrichment tool for animals and plants. *Bioinformatics* 36: 2628–2629.
- van der Graaff E, Dulk Ras AD, Hooykaas PJ, Keller B. 2000. Activation tagging of the LEAFY PETIOLE gene affects leaf petiole development in *Arabidopsis thaliana*. *Development* 127: 4971–4980.
- Gryffroy L, Ceulemans E, Manosalva Pérez N, Venegas-Molina J, Jaramillo-Madrid AC, Rodrigues SD, De Milde L, Jonckheere V, Van Montagu M, De Coninck B *et al.* 2023. Rhizogenic *Agrobacterium* protein RolB interacts with the TOPLESS repressor proteins to reprogram plant immunity and development. *Proceedings of the National Academy of Sciences, USA* 120: e2210300120.
- Gu Y, Wildermuth MC, Chakravarthy S, Loh Y, Yang C, He X, Han Y, Martin GB. 2002. Tomato transcription factors pti4, pti5, and pti6 activate defense responses when expressed in Arabidopsis. *Plant Cell* 14: 817–831.
- Han Q, Qi J, Hao G, Zhang C, Wang C, Dirk LMA, Downie AB, Zhao T. 2020. ZmDREB1A regulates RAFFINOSE SYNTHASE controlling raffinose accumulation and plant chilling stress tolerance in maize. *Plant and Cell Physiology* 61: 331–341.
- Hao D, Ohme-Takagi M, Sarai A. 1998. Unique mode of GCC box recognition by the DNA-binding domain of ethylene-responsive element-binding factor (ERF domain) in plant. *The Journal of Biological Chemistry* 273: 26857–26861.
- Harvey S, Kumari P, Lapin D, Griebel T, Hickman R, Guo W, Zhang R, Parker JE, Beynon J, Denby K *et al.* 2020. Downy Mildew effector HaRxL21 interacts with the transcriptional repressor TOPLESS to promote pathogen susceptibility. *PLoS Pathogens* 16: e1008835.
- He B, Shi P, Lv Y, Gao Z, Chen G. 2019. Gene coexpression network analysis reveals the role of SRS genes in senescence leaf of maize (*Zea mays* L.). *Journal of Genetics* 99: 3.
- Hiratsu K, Matsui K, Koyama T, Ohme Takagi M. 2003. Dominant repression of target genes by chimeric repressors that include the EAR motif, a repression domain, in Arabidopsis. *The Plant Journal* 34: 733–739.
- Hirota A, Kato T, Fukaki H, Aida M, Tasaka M. 2007. The auxin-regulated AP2/EREBP gene PUCHI is required for morphogenesis in the early lateral root primordium of Arabidopsis. *Plant Cell* 19: 2156–2168.
- Hu W, Ren Q, Chen Y, Xu G, Qian Y. 2021. Genome-wide identification and analysis of WRKY gene family in maize provide insights into regulatory network in response to abiotic stresses. *BMC Plant Biology* 21: 427.
- Hufford MB, Seetharam AS, Woodhouse MR, Chougule KM, Ou S, Liu J, Ricci WA, Guo T, Olson A, Qiu Y *et al.* 2021. *De novo* assembly, annotation, and comparative analysis of 26 diverse maize genomes. *Science* 373: 655–662.
- Jin J, Tian F, Yang DC, Meng YQ, Kong L, Luo J, Gao G. 2017. PLANTTFDB 4.0: toward a central hub for transcription factors and regulatory interactions in plants. *Nucleic Acids Research* 45: D1040–D1045.
- Kagale S, Rozwadowski K. 2011. EAR motif-mediated transcriptional repression in plants. *Epigenetics* 6: 141–146.
- Karim MR, Hirota A, Kwiatkowska D, Tasaka M, Aida M. 2009. A role for Arabidopsis PUCHI in floral meristem identity and bract suppression. *Plant Cell* 21: 1360–1372.
- Ke J, Ma H, Gu X, Thelen A, Brunzelle JS, Li J, Xu HE, Melcher K. 2015. Structural basis for recognition of diverse transcriptional repressors by the TOPLESS family of corepressors. *Science Advances* 1: e1500107.
- Khan M, Uhse S, Bindics J, Kogelmann B, Nagarajan N, Ingole KD, Djamei A. 2023. Tip of the iceberg? Three novel TOPLESS interacting effectors of the gall-inducing fungus *Ustilago maydis*. *Plant Biology*. doi: 10.1101/2023.06.12.544640.
- Komatsu M, Chujo A, Nagato Y, Shimamoto K, Kyojuka J. 2003. FRIZZY PANICLE is required to prevent the formation of axillary meristems and to establish floral meristem identity in rice spikelets. *Development* 130: 3841–3850.

- Koyama T, Nii H, Mitsuda N, Ohta M, Kitajima S, Ohme Takagi M, Sato F. 2013. A regulatory cascade involving class II ETHYLENE RESPONSE FACTOR transcriptional repressors operates in the progression of leaf senescence1. *Plant Physiology* 162: 991–1005.
- Krishnaswamy S, Verma S, Rahman MH, Kav NNV. 2011. Functional characterization of four APETALA2-family genes (RAP2.6, RAP2.6L, DREB19 and DREB26) in Arabidopsis. *Plant Molecular Biology* 75: 107–127.
- Kunst L, Klenz JE, Martinez-Zapater J, Haugbn GW. 1989. AP2 gene determines the identity of perianth organs in flowers of *Arabidopsis thaliana*. *Plant Cell* 1: 1195–1208.
- Lanver D, Müller AN, Happel P, Schweizer G, Haas FB, Franitz M, Pellegrin C, Reissmann S, Altmüller J, Rensing SA *et al.* 2018. The biotrophic development of *Ustilago maydis* studied by RNA-Seq analysis. *Plant Cell* 30: 300–323.
- Lee M-S, An J-H, Cho H-T. 2016. Biological and molecular functions of two EAR motifs of Arabidopsis IAA7. *Journal Of Plant Biology* 59: 24–32.
- Liao Y, Smyth GK, Shi W. 2014. FEATURECOUNTS: an efficient general purpose program for assigning sequence reads to genomic features. *Bioinformatics* 30: 923–930.
- Liu X, Galli M, Camehl I, Gallavotti A. 2019. RAMOSA1 ENHANCER LOCUS2-mediated transcriptional repression regulates vegetative and reproductive architecture. *Plant Physiology* 179: 348–363.
- Long JA, Ohno C, Smith ZR, Meyerowitz EM. 2006. TOPLESS regulates apical embryonic fate in Arabidopsis. *Science* 312: 1520–1523.
- Lorenzo O, Piqueras R, Sánchez Serrano JJ, Solano R. 2003. ETHYLENE RESPONSE FACTOR1 integrates signals from ethylene and jasmonate pathways in plant defense. *Plant Cell* 15: 165–178.
- Love MI, Huber W, Anders S. 2014. Moderated estimation of fold change and dispersion for RNA-seq data with DESeq2. *Genome Biology* 15: 1–21.
- Ma H, Duan J, Ke J, He Y, Gu X, Xu T, Yu H, Wang Y, Brunzelle JS, Jiang Y *et al.* 2017. A D53 repression motif induces oligomerization of TOPLESS corepressors and promotes assembly of a corepressor-nucleosome complex. *Science Advances* 3: e1601217.
- Ma Y, Yang C, He Y, Tian Z, Li J. 2017. Rice OVATE family protein 6 regulates plant development and confers resistance to drought and cold stresses. *Journal of Experimental Botany* 68: 4885–4898.
- Martin M. 2011. Cutadapt removes adapter sequences from high-throughput sequencing reads. *EMBnet Journal* 17(1): 10–12.
- Martin-Arevalillo R, Nanao MH, Larrieu A, Vinos-Poyo T, Mast D, Galvan-Ampudia C, Brunoud G, Vernoux T, Dumas R, Parcy F. 2017. Structure of the Arabidopsis TOPLESS corepressor provides insight into the evolution of transcriptional repression. *Proceedings of the National Academy of Sciences, USA* 114: 8107–8112.
- Maruyama Y, Yamoto N, Suzuki Y, Chiba Y, Yamazaki K, Sato T, Yamaguchi J. 2013. The Arabidopsis transcriptional repressor ERF9 participates in resistance against necrotrophic fungi. *Plant Science* 213: 79–87.
- Masaru OT, Hideaki S. 1995. Ethylene-inducible DNA binding proteins that interact with an ethylene-responsive element. *Plant Cell* 7: 173–182.
- Matei A, Ernst C, Günl M, Thiele B, Altmüller J, Walbot V, Usadel B, Doehlemann G. 2018. How to make a tumour: cell type specific dissection of *Ustilago maydis*-induced tumour development in maize leaves. *New Phytologist* 217: 1681–1695.
- McGrath KC, Dombrecht B, Manners JM, Schenk PM, Edgar CI, Maclean DJ, Scheible W-R, Udvardi MK, Kazan K. 2005. Repressor- and activator-type ethylene response factors functioning in jasmonate signaling and disease resistance identified via a genome-wide screen of Arabidopsis transcription factor gene expression. *Plant Physiology* 139: 949–959.
- Moffat CS, Ingle RA, Wathugala DL, Saunders NJ, Knight H, Knight MR. 2012. ERF5 and ERF6 play redundant roles as positive regulators of JA/Et-mediated defense against *Botrytis cinerea* in Arabidopsis. *PLoS ONE* 7: e35995.
- Mueller AN, Ziemann S, Treitschke S, Aßmann D, Doehlemann G. 2013. Compatibility in the *Ustilago maydis*-maize interaction requires inhibition of host cysteine proteases by the fungal effector Pit2. *PLoS Pathogens* 9: e1003177.
- Navarrete F, Gallei M, Kornienko AE, Saado I, Khan M, Chia K-SS, Darino MA, Bindics J, Djamei A. 2022. TOPLESS promotes plant immunity by repressing auxin signaling and is targeted by the fungal effector Naked1. *Plant Communications* 3: 100269.
- Oh E, Zhu JY, Ryu H, Hwang I, Wang ZY. 2014. TOPLESS mediates brassinosteroid-induced transcriptional repression through interaction with BZR1. *Nature Communications* 5: 1–12.
- Ohta M, Matsui K, Hiratsu K, Shinshi H, Ohme-Takagi M. 2001. Repression domains of class II ERF transcriptional repressors share an essential motif for active repression. *Plant Cell* 13: 1959–1968.
- Ohta M, Ohme Takagi M, Shinshi H. 2000. Three ethylene-responsive transcription factors in tobacco with distinct transactivation functions. *The Plant Journal* 22: 29–38.
- Ökmen B, Jaeger E, Schilling L, Finke N, Klemm A, Lee YJ, Wemhöner R, Pauly M, Neumann U, Doehlemann G. 2022. A conserved enzyme of smut fungi facilitates cell-to-cell extension in the plant bundle sheath. *Nature Communications* 13: 6003.
- Pauwels L, Barbero GF, Geerinck J, Tillemans S, Grunewald W, Pérez AC, Chico JM, Bossche RV, Sewell J, Gil E *et al.* 2010. NINJA connects the co-repressor TOPLESS to jasmonate signalling. *Nature* 464: 788–791.
- Perez-Riverol Y, Bai J, Bandla C, Garcia-Seisdedos D, Hewapathirana S, Kamathinathan S, Kundu DJ, Prakash A, Frericks-Zipper A, Eisenacher M *et al.* 2022. The PRIDE database resources in 2022: a hub for mass spectrometry-based proteomics evidences. *Nucleic Acids Research* 50: D543–D552.
- Pré M, Atallah M, Champion A, De Vos M, Pieterse CMJ, Memelink J. 2008. The AP2/ERF domain transcription factor ORA59 integrates jasmonic acid and ethylene signals in plant defense. *Plant Physiology* 147: 1347–1357.
- Rappsilber J, Ishihama Y, Mann M. 2003. Stop and go extraction tips for matrix-assisted laser desorption/ionization, nanoelectrospray, and LC/MS sample pretreatment in proteomics. *Analytical Chemistry* 75: 663–670.
- Redkar A, Doehlemann G. 2016. *Ustilago maydis* virulence assays in maize. *Bio-Protocol Journal* 6: e1760.
- Redkar A, Hoser R, Schilling L, Zechmann B, Krzymowska M, Walbot V, Doehlemann G. 2015. A secreted effector protein of *Ustilago maydis* guides maize leaf cells to form tumors. *Plant Cell* 27: 1332–1351.
- Robinson MD, McCarthy DJ, Smyth GK. 2010. EDGER: a Bioconductor package for differential expression analysis of digital gene expression data. *Bioinformatics* 26: 139–140.
- Rushton PJ, Somssich IE, Ringler P, Shen QJ. 2010. WRKY transcription factors. *Trends in Plant Science* 15: 247–258.
- Sakuma Y, Liu Q, Dubouzet JG, Abe H, Shinozaki K, Yamaguchi-Shinozaki K. 2002. DNA-binding specificity of the ERF/AP2 domain of Arabidopsis DREBs, transcription factors involved in dehydration- and cold-inducible gene expression. *Biochemical and Biophysical Research Communications* 290: 998–1009.
- Schilling L, Matei A, Redkar A, Walbot V, Doehlemann G. 2014. Virulence of the maize smut *Ustilago maydis* is shaped by organ-specific effectors. *Molecular Plant Pathology* 15: 780–789.
- Schuster M, Schweizer G, Kahmann R. 2018. Comparative analyses of secreted proteins in plant pathogenic smut fungi and related basidiomycetes. *Fungal Genetics and Biology* 112: 21–30.
- Sessa G, Meller Y, Fluhr R. 1995. A GCC element and a G-box motif participate in ethylene-induced expression of the PRB-1b gene. *Plant Molecular Biology* 28: 145–153.
- Skibbe DS, Doehlemann G, Fernandes J, Walbot V. 2010. Maize tumors caused by *Ustilago maydis* require organ-specific genes in host and pathogen. *Science* 328: 89–92.
- Solano R, Stepanova A, Chao Q, Ecker JR. 1998. Nuclear events in ethylene signaling: a transcriptional cascade mediated by ETHYLENE-INSENSITIVE3 and ETHYLENE-RESPONSE-FACTOR1. *Genes & Development* 12: 3703–3714.
- Sun X, Ma Y, Yang C, Li J. 2020. Rice OVATE family protein 6 regulates leaf angle by modulating secondary cell wall biosynthesis. *Plant Molecular Biology* 104: 249–261.
- Szemenyei H, Hannon M, Long JA. 2008. TOPLESS mediates auxin-dependent transcriptional repression during Arabidopsis embryogenesis. *Science* 319: 1384–1386.

- Tian F, Yang D-C, Meng Y-Q, Jin J, Gao G. 2020. PLANTREGMAP: charting functional regulatory maps in plants. *Nucleic Acids Research* 48: D1104–D1113.
- Tyanova S, Temu T, Cox J. 2016. The MAXQUANT computational platform for mass spectrometry-based shotgun proteomics. *Nature Protocols* 11: 2301–2319.
- Wang C, Yang Q, Yang Y. 2011. Characterization of the ZmDBP4 gene encoding a CRT/DRE-binding protein responsive to drought and cold stress in maize. *Acta Physiologiae Plantarum* 33: 575–583.
- Wang S, Chang Y, Guo J, Chen J-G. 2007. Arabidopsis Ovate Family Protein 1 is a transcriptional repressor that suppresses cell elongation. *The Plant Journal* 50: 858–872.
- Wiśniewski JR, Zougman A, Mann M. 2009. Combination of FASP and StageTip-based fractionation allows in-depth analysis of the hippocampal membrane proteome. *Journal of Proteome Research* 8: 5674–5678.
- Wu A, Allu AD, Garapati P, Siddiqui H, Dortay H, Zanol MI, Asensi Fabado MA, Munné Bosch S, Antonio C, Tohge T *et al.* 2012. JUNGBRUNNEN1, a reactive oxygen species-responsive NAC transcription factor, regulates longevity in Arabidopsis. *Plant Cell* 24: 482–506.
- Zhang Y, Von Behrens I, Zimmermann R, Ludwig Y, Hey S, Hochholdinger F. 2015. LATERAL ROOT PRIMORDIA 1 of maize acts as a transcriptional activator in auxin signalling downstream of the Aux/IAA gene rootless with undetectable meristem 1. *Journal of Experimental Botany* 66: 3855–3863.
- Zuo W, Depotter JRL, Gupta DK, Thines M, Doehlemann G. 2021. Cross-species analysis between the maize smut fungi *Ustilago maydis* and *Sporisorium reilianum* highlights the role of transcriptional change of effector orthologs for virulence and disease. *New Phytologist* 232: 719–733.

Supporting Information

Additional Supporting Information may be found online in the Supporting Information section at the end of the article.

Dataset S1 Differential expression analysis of Δ Tip6 vs SG200-infected *Zea mays* using DESEQ2.

Dataset S2 Differential expression analysis of Tip6EARm vs SG200-infected *Zea mays* using DESEQ2.

Dataset S3 Differential expression analysis of Δ Tip6 vs SG200-infected *Zea mays* using EDGER.

Dataset S4 Differential expression analysis of Tip6EARm vs SG200-infected *Zea mays* using EDGER.

Dataset S5 Overlay differential expression genes of Δ Tip6 vs SG200-infected *Zea mays* using DESEQ2 and EDGER.

Dataset S6 Overlay differential expression genes of Tip6EARm vs SG200-infected *Zea mays* using DESEQ2 and EDGER.

Dataset S7 Annotated differentially expressed genes: Δ Tip6 vs SG200 for Gene Ontology analysis.

Dataset S8 Differential expression transcription factors of Δ Tip6 vs SG200-infected *Zea mays*.

Dataset S9 Annotated differentially expressed genes: Tip6EARm vs SG200 for Gene Ontology analysis.

Dataset S10 Differential expression transcription factors of Tip6EARm vs SG200-infected *Zea mays*.

Dataset S11 Enriched transcription factors regulating differentially expressed genes: Δ Tip6 vs SG200 comparison.

Dataset S12 Prediction of potential transcription factors regulating differentially expressed genes: Δ Tip6 vs SG200 comparison.

Dataset S13 Enriched transcription factors regulating differentially expressed genes: Tip6EARm vs SG200 comparison.

Dataset S14 Prediction of potential transcription factors regulating differentially expressed genes: Tip6EARm vs SG200 comparison.

Fig. S1 Co-immunoprecipitation to identify host interaction targets.

Fig. S2 Western blot confirmation of Tip6 expression alongside maize TPL proteins.

Fig. S3 Purification of mCherry, Tip6-mCherry, and 6xHis-RELK2^N-6xHis by size-exclusion chromatography.

Fig. S4 Absence of interaction between Tip6 Δ EARs and RELK2.

Fig. S5 Conservation of EAR motifs in UmTip6 orthologs and interaction between SrTip6 and maize TPL family proteins.

Fig. S6 Subcellular localization of RELK2 in *Nicotiana benthamiana* and *Zea mays*.

Fig. S7 Subcellular localization of RELK1 and RELK3, and their co-expression with Tip6 in *Nicotiana benthamiana* leaves.

Fig. S8 Overview of differentially expressed gene analysis.

Fig. S9 Enriched transcription factors regulate differentially expressed genes.

Table S1 Oligonucleotides and plant infection disease symptom scoring in this study.

Table S2 Mass spectrometry data of Tip6 in *Nicotiana benthamiana*.

Table S3 Mass spectrometry data of Tip6 in *Zea mays*.

Please note: Wiley is not responsible for the content or functionality of any Supporting Information supplied by the authors. Any queries (other than missing material) should be directed to the *New Phytologist* Central Office.